Spherical Wavelets Applied to the Analysis of the Cosmic Microwave Background Anisotropies

Enrique Martínez González
Instituto de Física de Cantabria

MGA IV, 8-12 November 2004

IPAM, Los Angeles, CA

LAYOUT

- Introduction
- Description of CMB anisotropies
- Physics of anisotropies
- Cosmological parameters
- Observations and problematics
- Analysis of the CMB using Spherical Wavelets:
    - Extragalactic point sources
    - Non-Gaussianity
    - Integrated Sachs-Wolfe Effect
- Conclusions

CMB electromagnetic spectrum

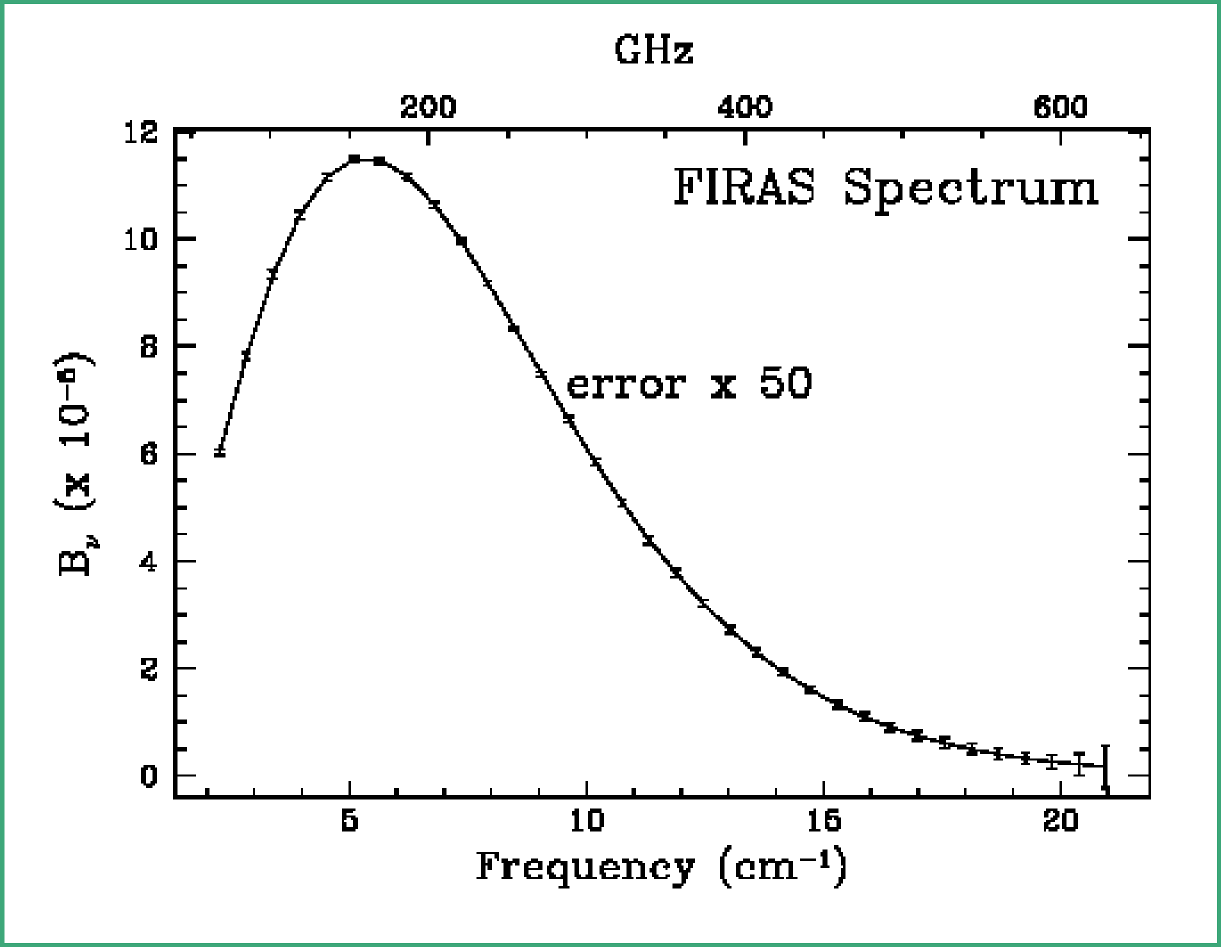

$T = 2.728 \pm 0.004$ K

CMB anisotropies

• The cosmological model determines the statistical properties

• The fluctuations are expanded in spherical harmonics:

$$\frac{\Delta T}{T}(\vec{n}) = \sum_{\ell=1}^{\infty} \sum_{m=-\ell}^{\ell} a_{\ell m} Y_{\ell m}(\vec{n}) \qquad \ell \approx \frac{1}{\theta}$$

• If the fluctuations are Gaussian the statistical properties are completely characterized by the power spectrum C_l (no dependence on "m" because of isotropy).

RADIATION POWER SPECTRUM C_l

- $C(\theta)$-C_l relationship:

$$C(\theta) = \langle \Delta T(\vec{n}_1)\Delta T(\vec{n}_2)\rangle = \sum_l \frac{2l+1}{4\pi} C_l W_l P_l(\cos\theta)$$

$$C_l \equiv \langle |a_{lm}|^2 \rangle = \frac{\sum_m |a_{lm}|^2}{2l+1}$$

- The power per logarithmic interval ΔT_l^2 is usually displayed:

$$\Delta T_l^2 = \frac{l(l+1)}{2\pi} C_l T^2$$

- Fundamental limitation to measure C_l (cosmic variance):

$$\frac{\Delta C_l}{C_l} = \frac{1}{\sqrt{l+1/2}} f_{sky}^{-1/2}$$ (Gaussian case)

(Scott et al. 1994)

DYNAMICS OF THE UNIVERSE

The dynamics of the universe are characterized by two equations:

Acceleration = - GM/R^2 ~ - (_+3p)R

Equation of state: p=w _

Dynamical phases in the history of the universe:

- Inflation (10^{-35} s): p=-_ (w=-1), accel. ~ +2_R → "Repulsion" Acceleration
- Radiation dominated (z>3200): p=_/3 (w=1/3) → Deceleration
- Matter dominated (z<3200): p=0 (w=0) → Deceleration
- Dark energy dominated (z<0.5): p=-_ (w=-1) → Acceleration

COSMOLOGICAL PARAMETERS

- Background universe

- H_0: expansion rate
- $\_{tot}$: density parameters = $\_R + \_B + \_\nu + \_{CDM} + \_{DE}$
- w: equation of state parameter: $p=w\rho$
- τ: reionization optical depth: $\tau = \sigma_T \int_{t_i}^{t_o} n_e(t)\,dt$

- Initial fluctuation spectrum ($P(k)=Ak^{n(k)}$)

- A_s: scalar amplitude at k=0.05/Mpc
- n_s: scalar index at k=0.05/Mpc
- α: running = dn/dlnk
- r: tensor-to-scalar ratio = A_t/A_s
- n_t: tensor index = -r/8 ← Inflation (consistency relation)

THE CMB AND THE LSS

CMB

EVOLUTION

Adiabatic fluctuations

Physical effects producing anisotropies

$$\frac{\Delta T}{T}(\vec{n}) = \left(\frac{\Delta T}{T}(\vec{n})\right)_d + \frac{1}{3}\phi_d + \int \frac{\partial \phi}{\partial t} dt + \vec{n} \cdot (\vec{v}_0 - \vec{v}_d)$$

Temperature = Intrinsic fluctuation + Gravity + Gravitational potential variation + Velocity

PRIMARY ANISOTROPIES

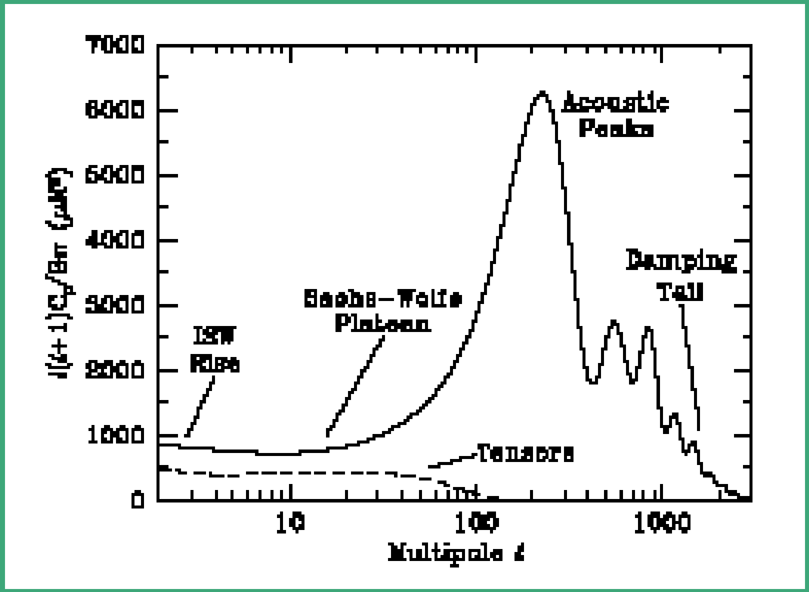

(Scott & Smoot 2004)

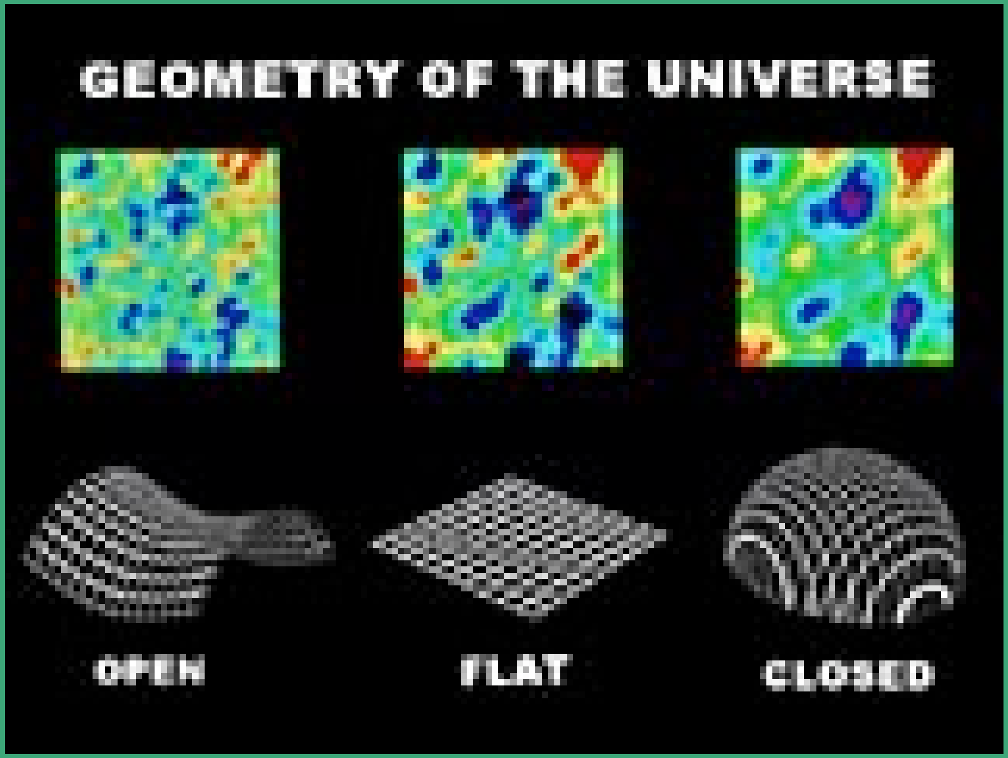
GEOMETRY OF THE UNIVERSE
OPEN
FLAT
CLOSED

Measurement of cosmological parameters with CMB

Temperature Angular spectrum varies with:

Ω_{tot} , Ω_b , Ω_{CDM}, Ω_{DE}, τ, n_s, h, A_s, r,

(CMBFAST, CAMB)

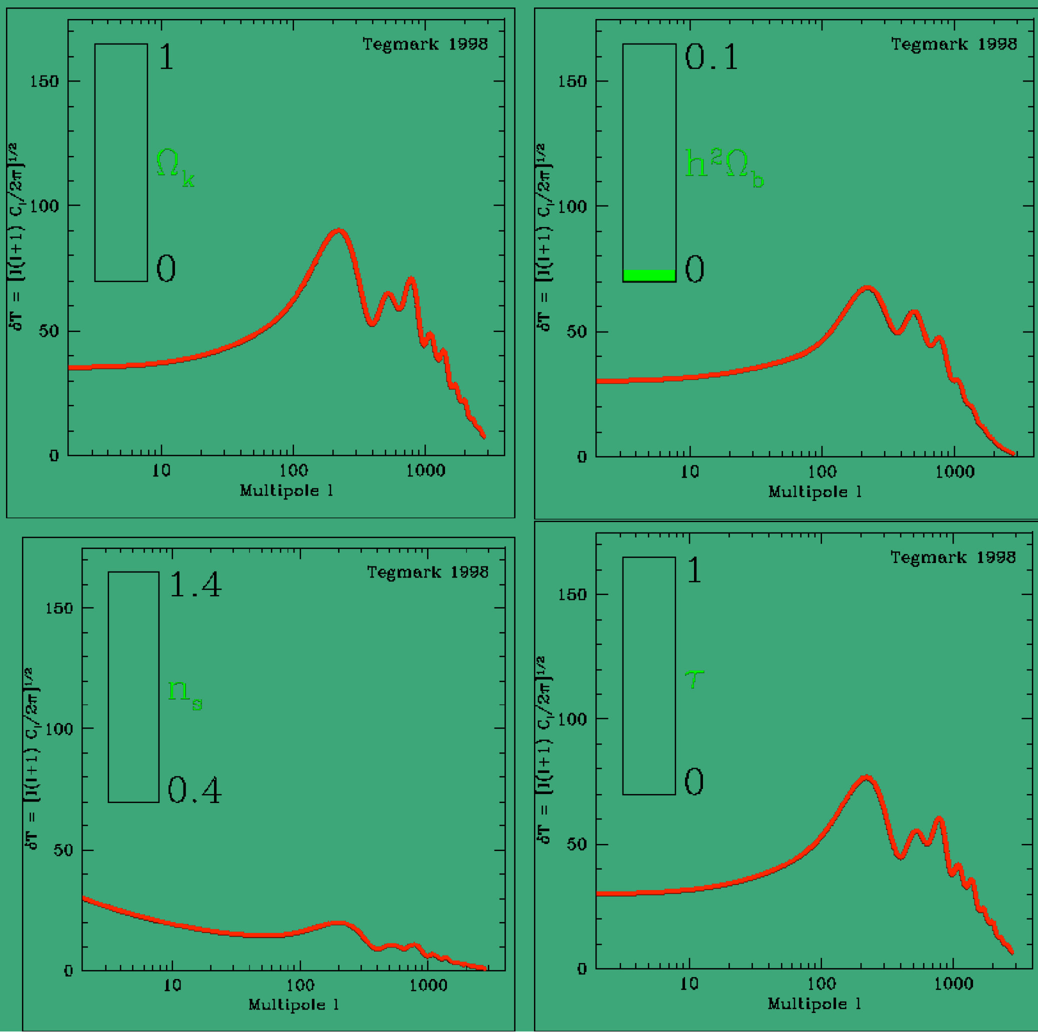

. . . .

SECONDARY ANISOTROPIES

(Hu & Dodelson 2002)

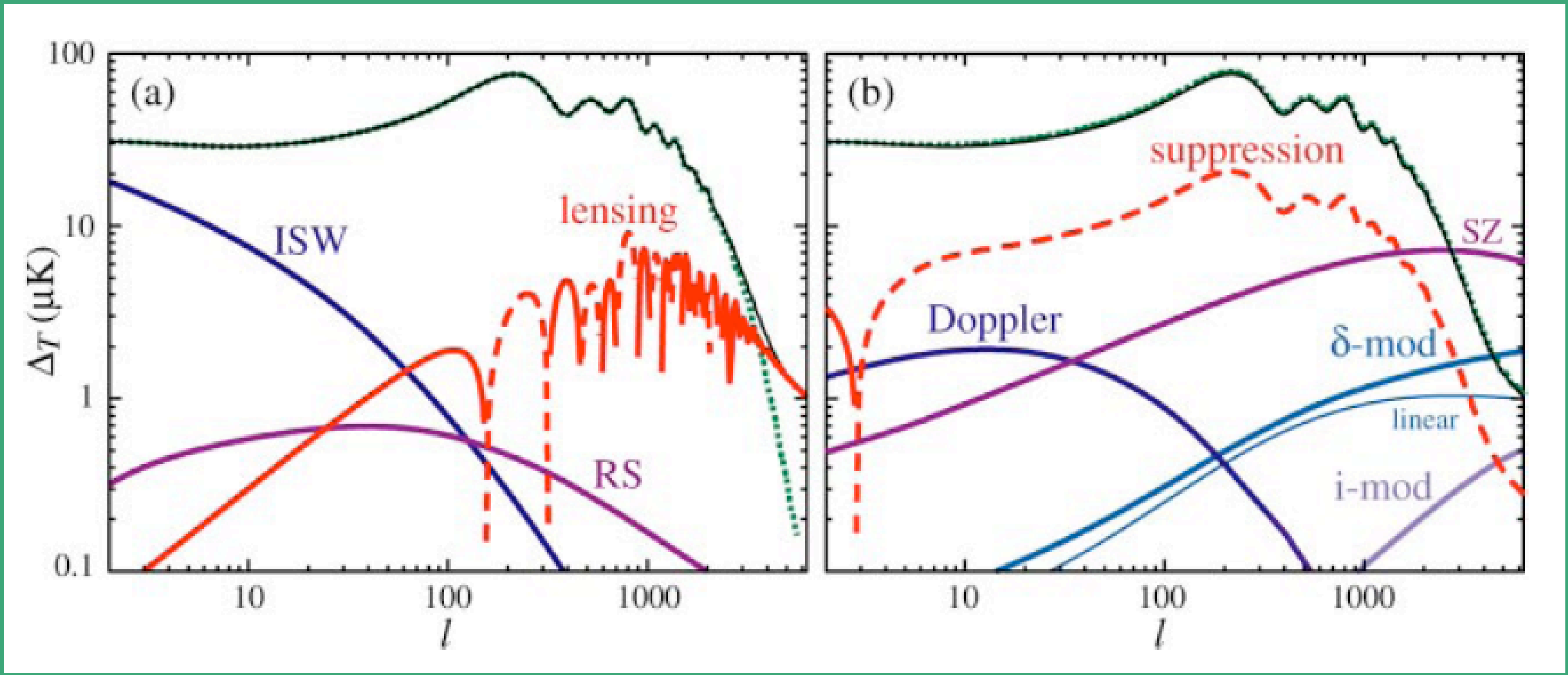

FOREGROUNDS

- Different Galactic and extragalactic foregrounds emit in mm wavelengths obstructing the observation of the CMB.
- Galactic foregrounds produce fluctuations with relatively more power on large scales ($C_l \propto l^{-3}$) and are due to synchrotron emission ($T_A \propto \nu^{-3}$), free-free ($T_A \propto \nu^{-2}$) and thermal dust ($I_\nu \propto \nu^2 B_\nu(T_D)$, with $T_D \sim$ 10-20K).
- Extragalactic radio and IR sources are important at low and high frequency limits of the mm band.
- Thermal Sunyaev-Zeldovich emission from hot gas in clusters produces negative/positive temperature fluctuations below/above $\approx$ 220 GHz. Kinetic SZ effect is a factor $\approx$ 30 smaller but a blackbody frequency dependence.
- Evidences of the presence of aditional Galactic foregrounds (spining dust?) have been recently claimed (Oliveira-Costa et al. 2004).

FREE-FREE

(Bennett et al. 2004)

Hα (Finkbeiner 2003)

WMAP K-band

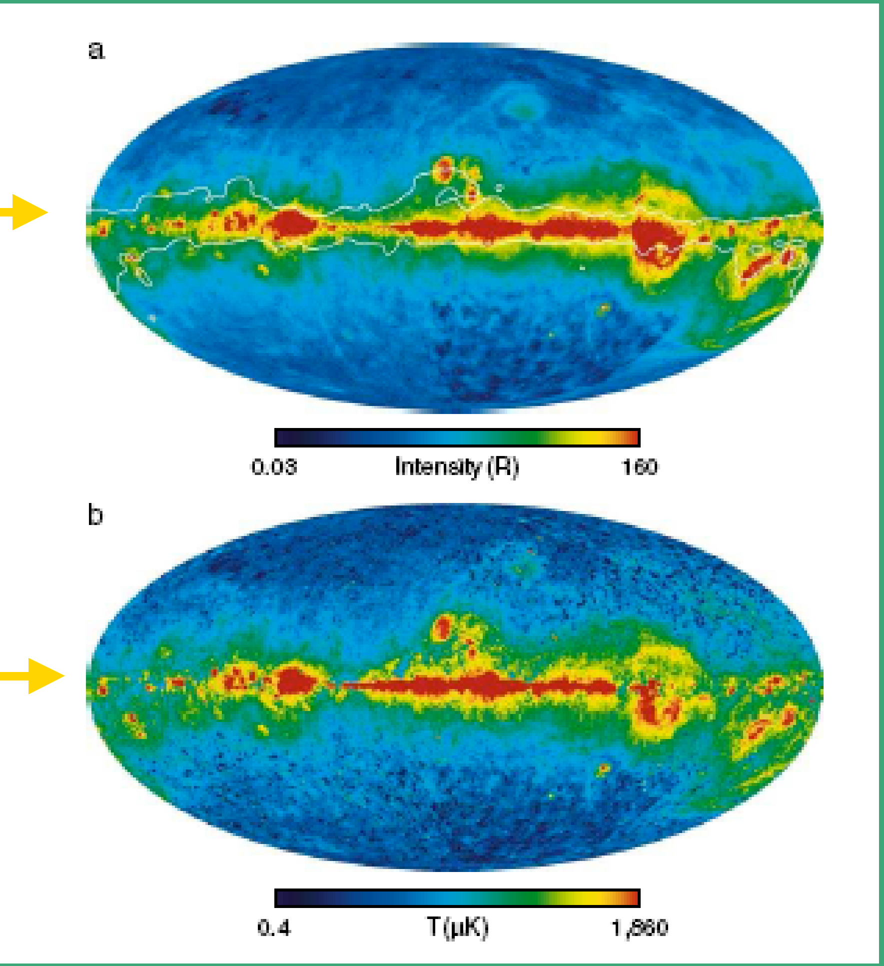

SYNCHROTRON

(Bennett et al. 2004)

Haslam 408MHz

WMAP K-band

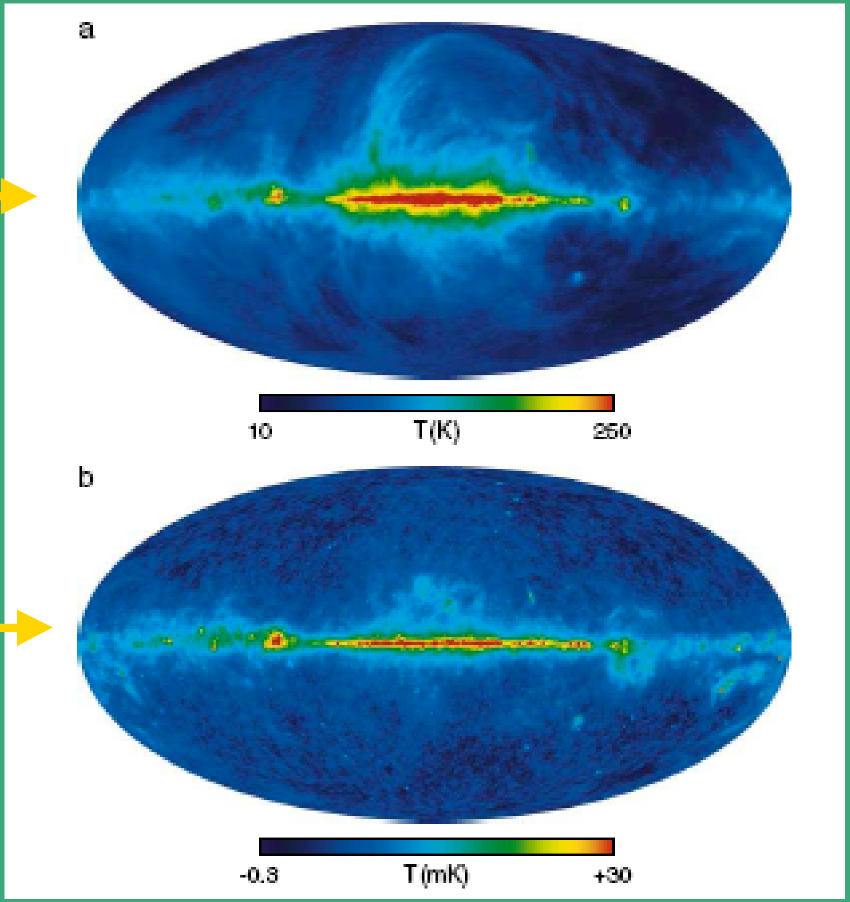

THERMAL DUST

(Bennett et al. 2004)

Finkbeiner et al. 99

(94GHz)

WMAP Wband

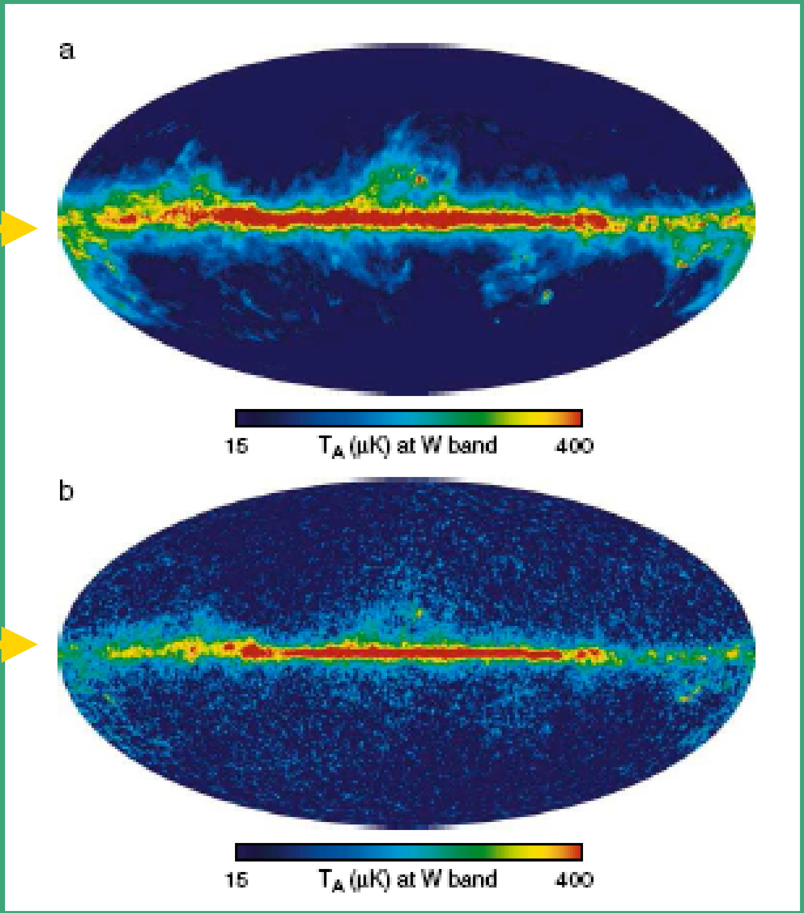

CMB versus Galactic foregrounds

(Bennett et al. 2004)

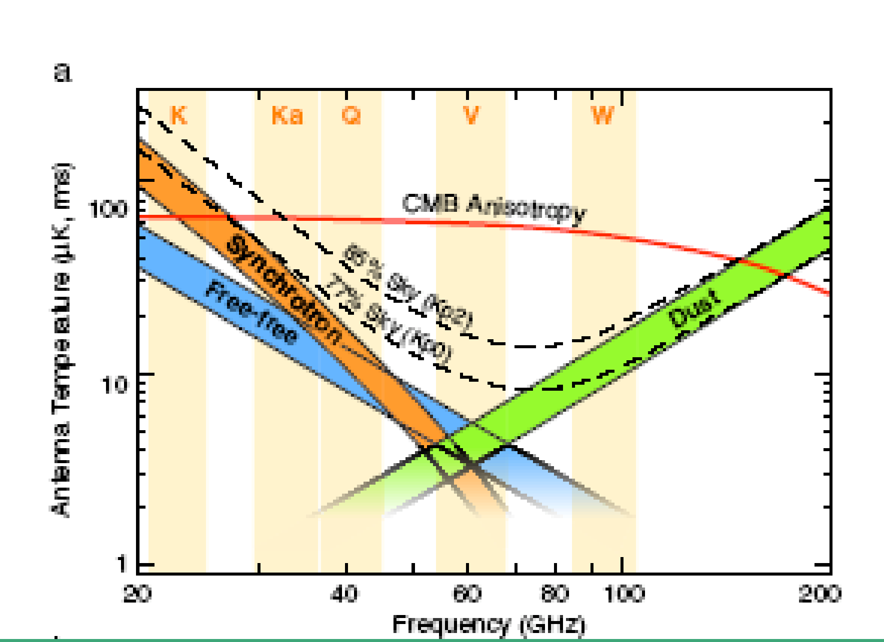

DATA PIPELINE AND COMPRESSION

(Hu & Dodelson 2002)

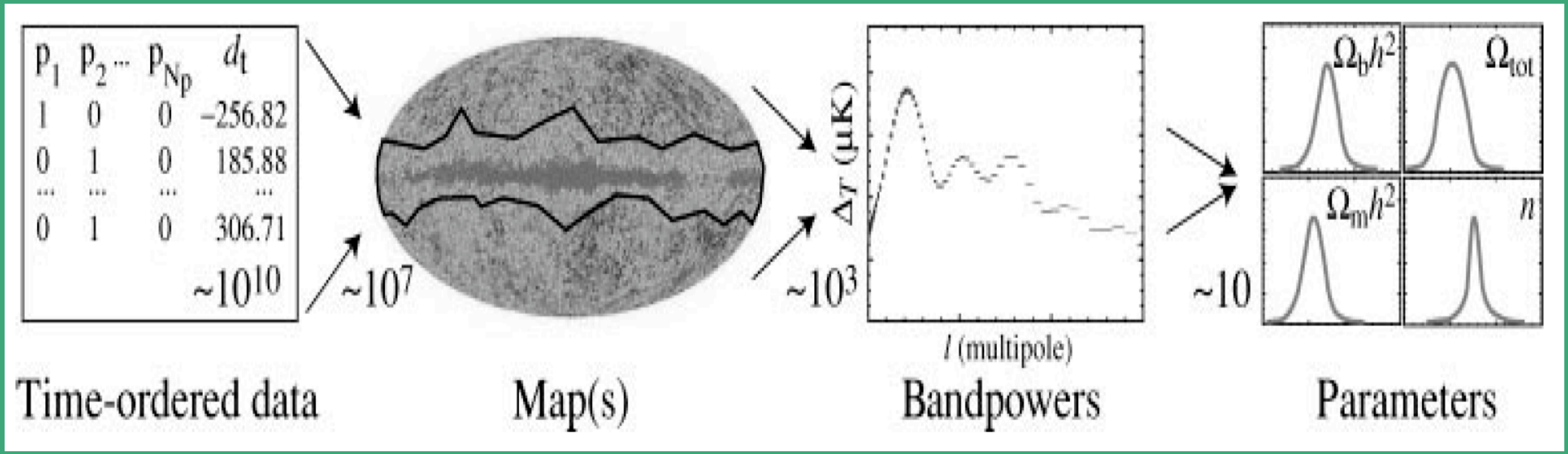

Wilkinson Microwave Anisotropy Probe

A partnership between NASA/GSFC and Princeton

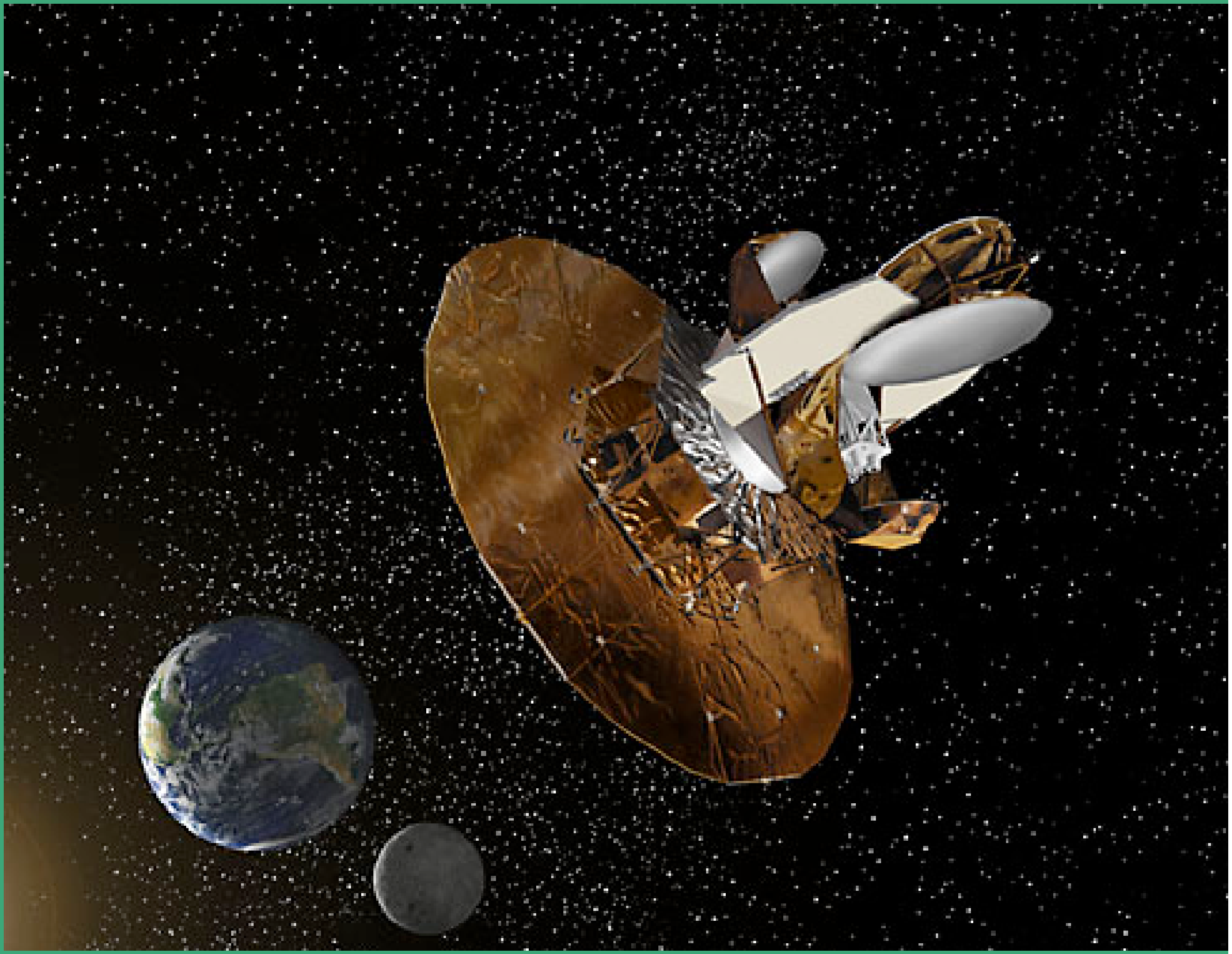

Science Team:

NASA/GSFC

Chuck Bennett (**PI**)
Michael Greason
Bob Hill
Gary Hinshaw
Al Kogut
Michele Limon
Nils Odegard
Janet Weiland
Ed Wollack

Brown

Greg Tucker

UCLA

Ned Wright

UBC

Mark Halpern

Chicago

Stephan Meyer

Princeton

Chris Barnes
Norm Jarosik
Eiichiro Komatsu
Michael Nolta
Lyman Page
Hiranya Peiris
David Spergel
Licia Verde

Table 1. Approximate Observational Properties by Band

Item	K-Band	Ka-Band	Q-Band	V-Band	W-Band
Wavelength, λ (mm)	13	9.1	7.3	4.9	3.2
Frequency, ν (GHz)	22.8	33.0	40.7	60.8	93.5
Ant./therm. conversion factor, $\Delta T/\Delta T_A$	1.014	1.029	1.044	1.100	1.251
Noise, σ_0 (mK) $\sigma = \sigma_0 N_{obs}^{-1/2}$	1.424	1.449	2.211	3.112	6.498
Beam width θ(°FWHM)	0.82	0.62	0.49	0.33	0.21
No. of Differencing Assemblies	1	1	2	2	4
No. of Radiometers	2	2	4	4	8
No. of Channels	4	4	8	8	16

WMAP (1st year maps)

Galactic foreground monitors

K-band (23 GHz)

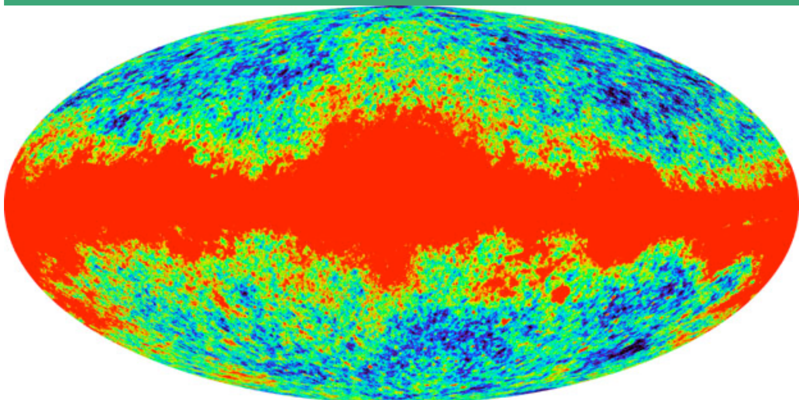

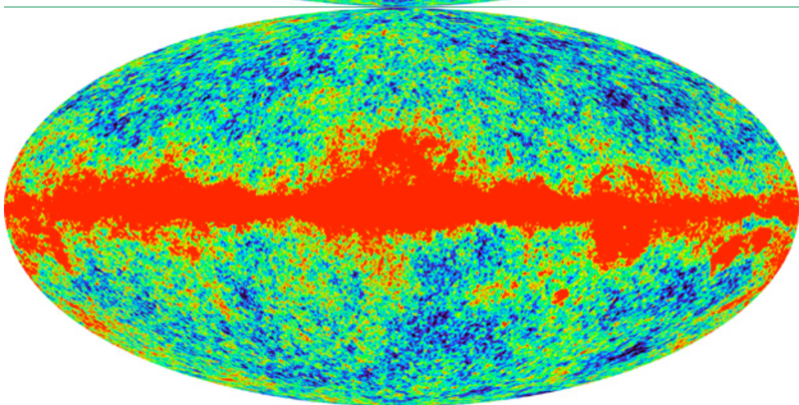

Ka-band (33 GHz)

CMB bands

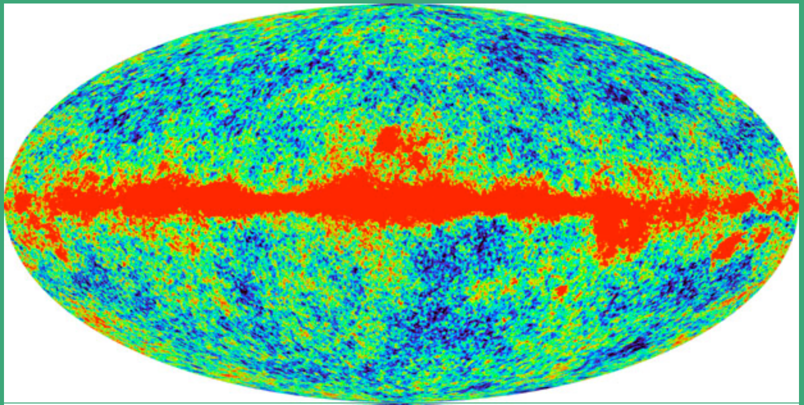

Q-band (41 GHz)

2 channels

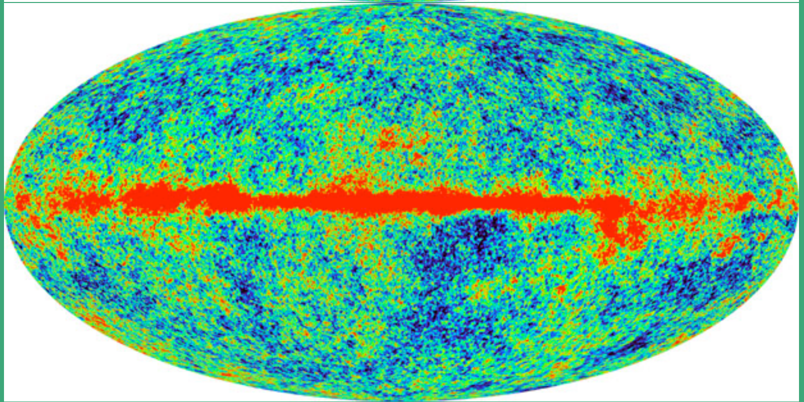

V-band (61 GHz)

2 channels

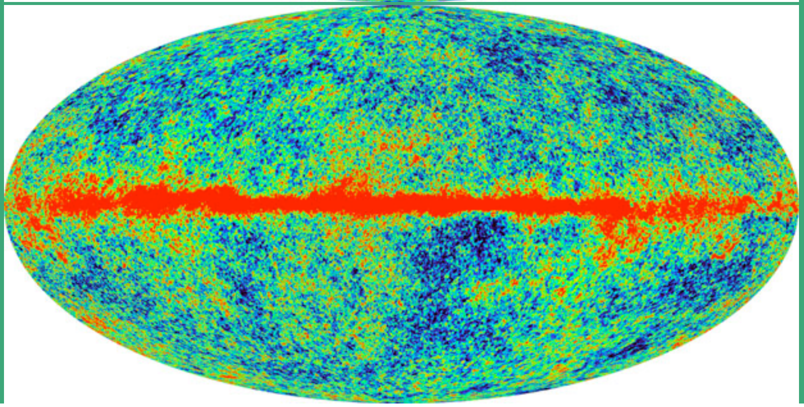

W-band (93 GHz)

4 channels

WMAP C_l (TT, TE)

TT

TE

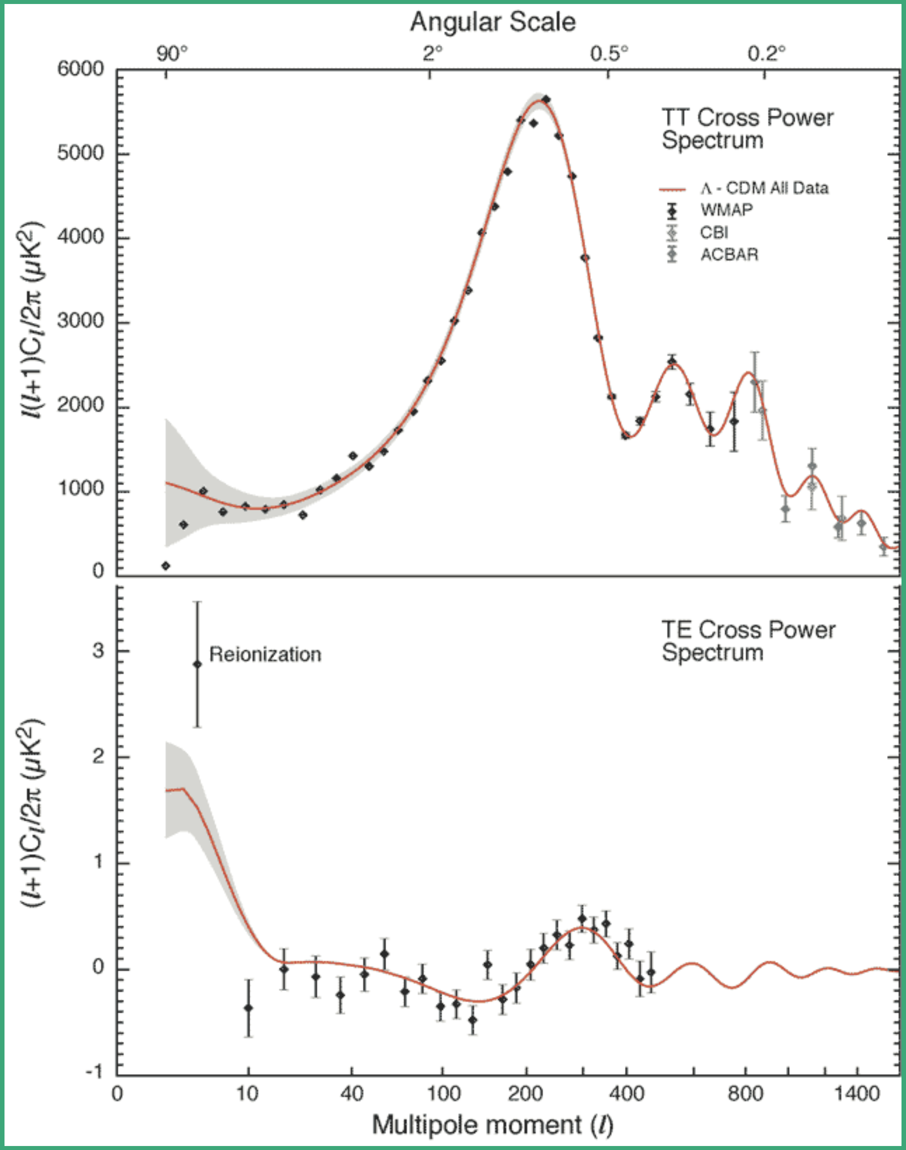

WMAP data only

(Spergel et al. 03)

Table 1. Power Law ΛCDM Model Parameters- *WMAP* Data Only **(τ<0.3)**

Parameter		Mean (68% confidence range)	Maximum Likelihood
Baryon Density	$\Omega_b h^2$	0.024 ± 0.001	0.023
Matter Density	$\Omega_m h^2$	0.14 ± 0.02	0.13
Hubble Constant	h	0.72 ± 0.05	0.68
Amplitude	A	0.9 ± 0.1	0.78
Optical Depth	τ	$0.166^{+0.076}_{-0.071}$	0.10
Spectral Index	n_s	0.99 ± 0.04	0.97
	χ^2_{eff}/ν		1431/1342

[a]Fit to *WMAP* data only

- **Consistent with the concordance (“benchmark”) model**
- **Einstein-de Sitter model is rejected at > 5σ !**

THE PLANCK MISSION

- European mission to map the Cosmic Microwave Background (CMB)
- Its main observational objective is to image the whole sky at wavelengths near the intensity peak of the CMB radiation, with high instrument sensitivity ($\Delta T/T \sim 10^{-6}$) and resolution ($\approx$5 arcmin), wide frequency coverage (25 GHz-950 GHz) and high control of systematics.
- Launch: 2007
- Payload module: 2 instruments and telescope
- Instruments::
  - Low Frequency Instrument (LFI, HEMTs)
  - High Frequency Instrument (HFI, bolometers)
- Telescope: primary (1.50x1.89 m ellipsoid) and secondary (1.02x1.04 m)

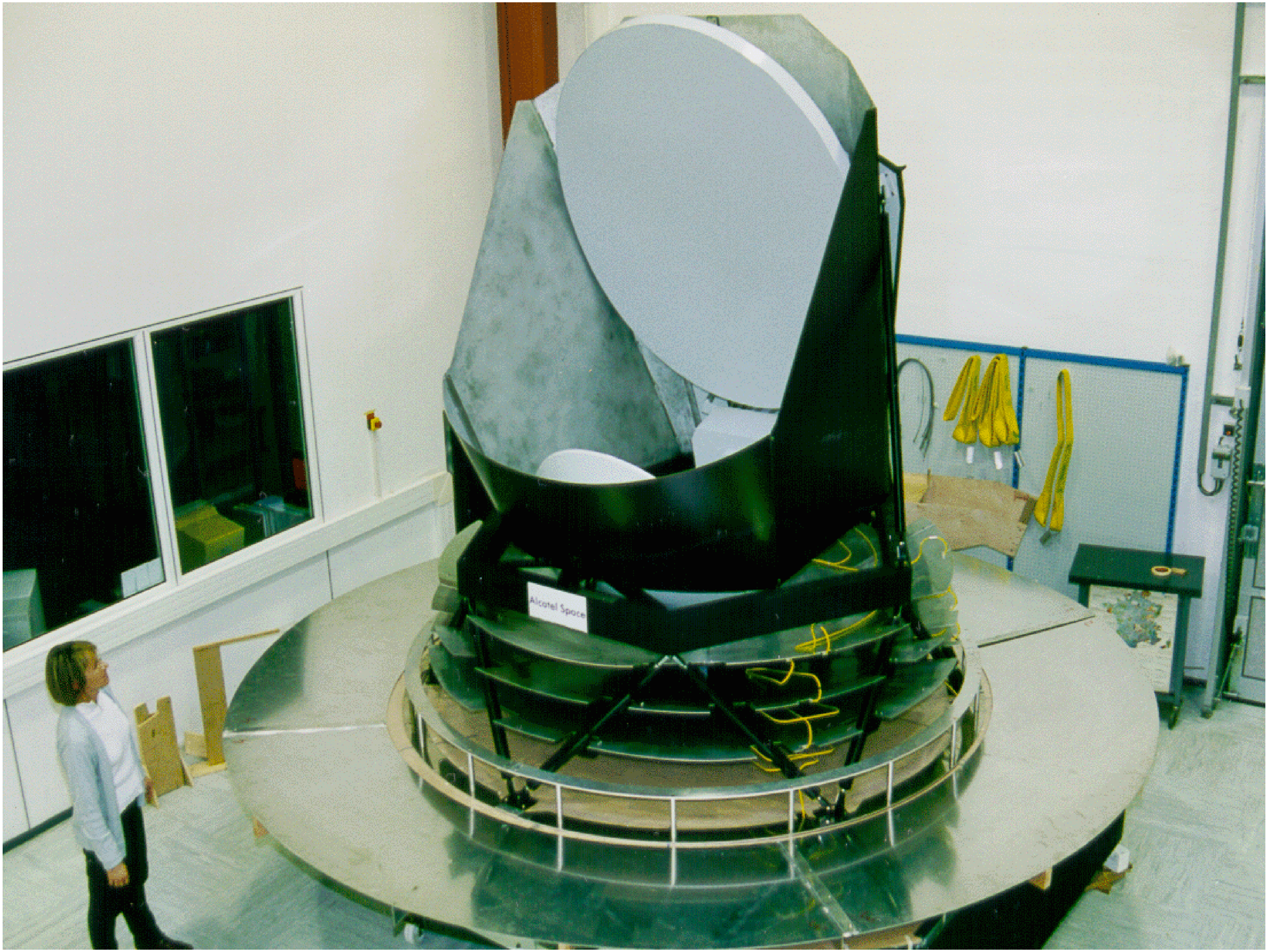
Alcatel Space

Observing strategy

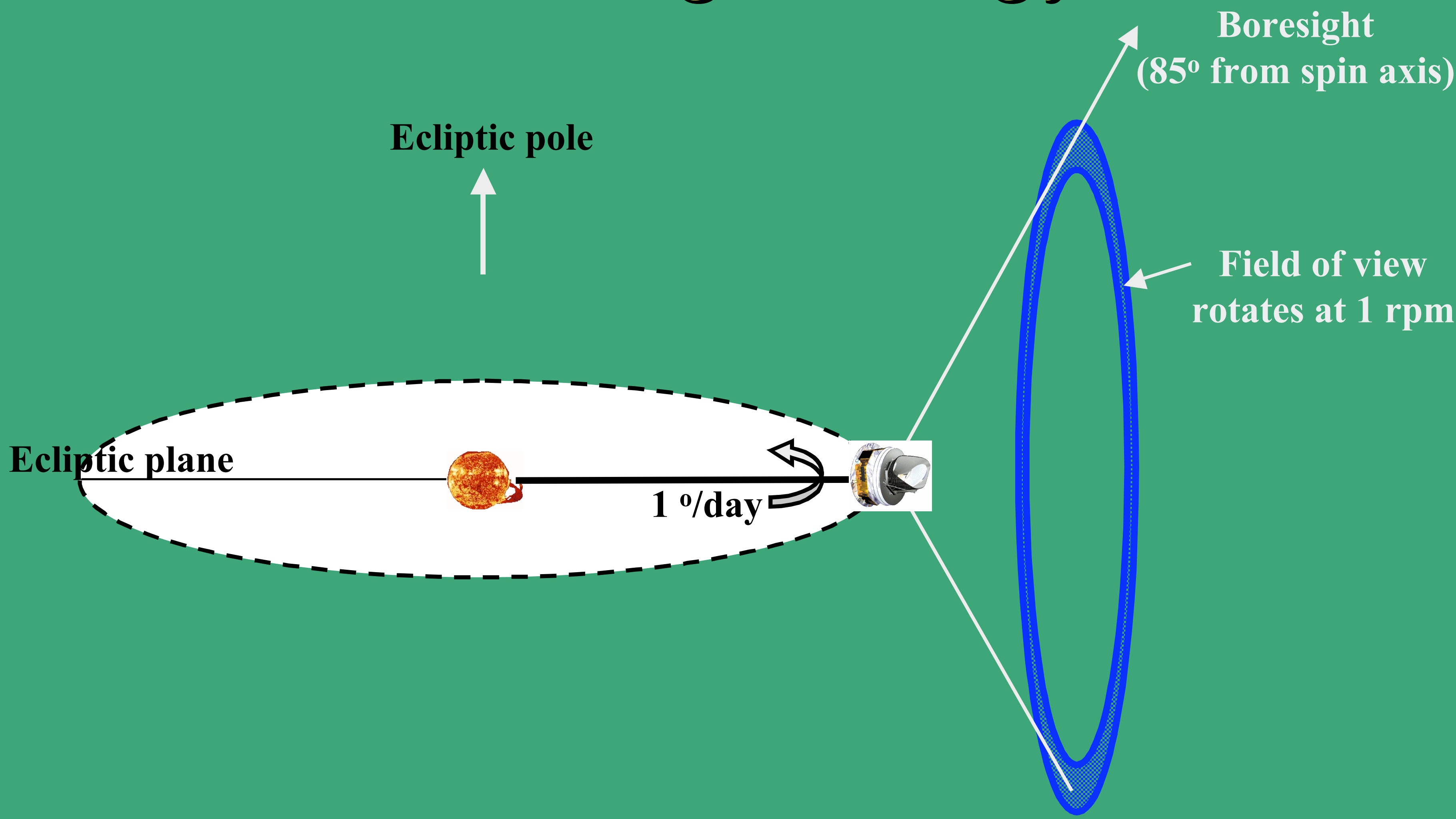

Estimated Instrument Performance Goals

Telescope	1.5 m (proj. aperture) aplanatic; shared focal plane; system emissivity 1%								
	Viewing direction offset 85° from spin axis; Field of View 8°								
Instrument	LFI			HFI					
Center Freq. (GHz)	30	44	70	100	143	217	353	545	857
Detector Technology	HEMT LNA arrays			Bolometer arrays					
Detector Temperature	~20 K			0.1 K					
Cooling Requirements	H_2 sorption cooler			H_2 sorption + 4 K J-T stage + Dilution cooler					
Number of Unpol. Detectors	0	0	0	0	4	4	4	4	4
Number of Linearly Polarised Detectors	4	6	12	8	8	8	8	0	0
Angular Resolution (FWHM, arcmin)	33	24	14	9.5	7.1	5	5	5	5
Bandwidth (GHz)	6	8.8	14	33	47	72	116	180	283
Average $\Delta T/T_I{}^*$ per pixel#	2.0	2.7	4.7	2.5	2.2	4.8	14.7	147	6700
Average $\Delta T/T_{U,Q}{}^*$ per pixel#	2.8	3.9	6.7	4.0	4.2	9.8	29.8		

* Sensitivity (1σ) to intensity (Stokes I) fluctuations observed on the sky, in thermodynamic temperature ($x10^{-6}$) units, relative to the average temperature of the CMB (2.73 K), achievable after two sky surveys (14 months).

A pixel is a square whose side is the FWHM extent of the beam.

* Sensitivity (1σ) to polarised intensity (Stokes U and Q) fluctuations observed on the sky, in thermodynamic temperature ($x10^{-6}$) units, relative to the average temperature of the CMB (2.73 K), achievable after two sky surveys (14 months).

Table last updated Feb. 2004

WMAP vs Planck: **Key differences**

	WMAP	Planck
P/L Technology	Dual telescope Passive cooling	Single telescope Active cooling
Detectors	HEMT LNAs	HEMT LNAs Bolometers
Freq. range	22-94 GHz	30-857 GHz
Ang. resolution	13.8 arcmin	5 arcmin
Sensitivity @ 90-100 GHz	35 μK ($0^o.3 \times 0^o.3$)	2.2 μK ($0^o.3 \times 0^o.3$)
Sensitivity to CMB (after avg. & fg. Subtr.)	Min. 31 μK Typ. 35 μK	Min. 3 μK Typ. 5 μK

WMAP-PLANCK

Temperature

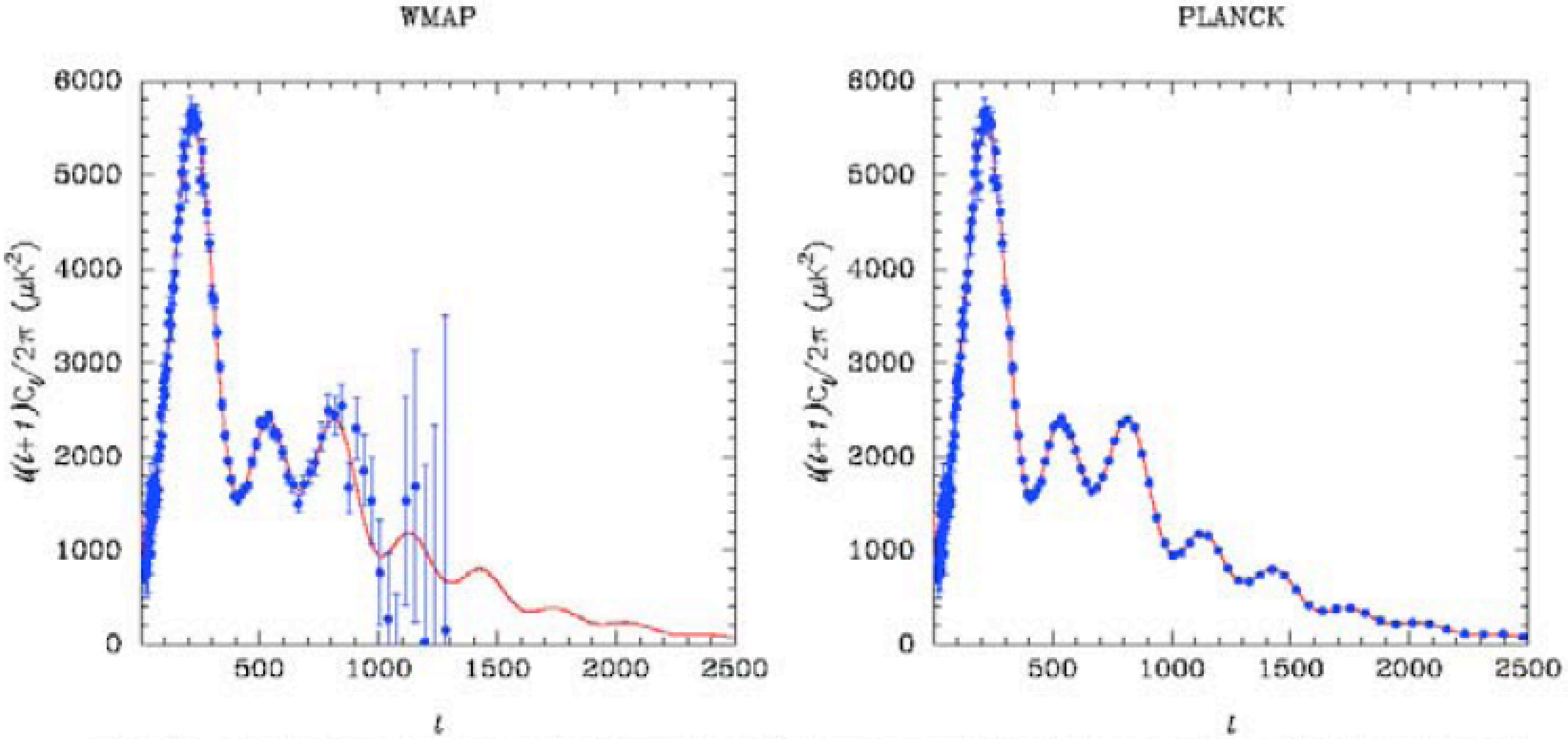

FIG 2.8.—The left panel shows a realisation of the CMB power spectrum of the concordance ΛCDM model (red line) after 4 years of *WMAP* observations. The right panel shows the same realisation observed with the sensitivity and angular resolution of *Planck*.

From: Efstathiou 2004

WMAP-PLANCK

E-mode polarization

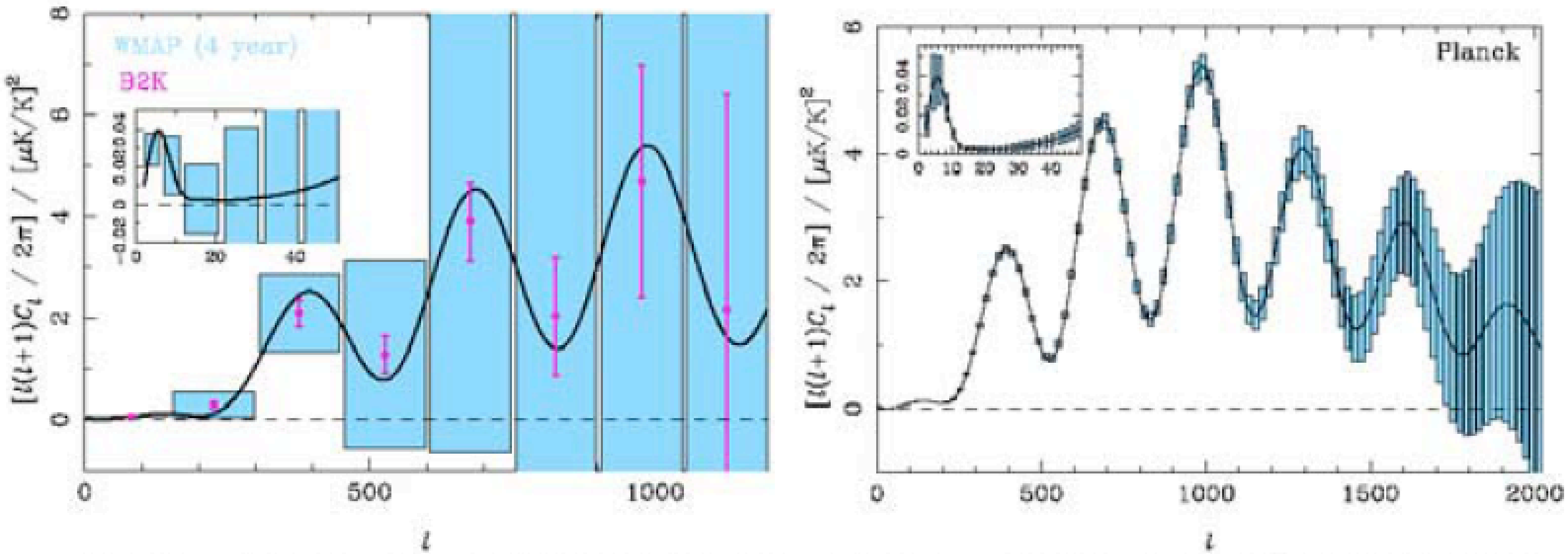

FIG 2.14.—Forecasts for the $\pm1\sigma$ errors on the E-mode polarization power spectrum C_ℓ^E from *WMAP* and B2K (left) and *Planck* (right). The cosmological model, and the assumptions about instrument characteristics, are the same as in Fig. 2.13. For *WMAP* and B2K, flat band powers are estimated with $\Delta\ell = 150$ (with finer resolution on large scales for *WMAP* in the inset). For *Planck* we have used the same ℓ-resolution as in Fig. 2.13.

From: Efstathiou 2004

B-mode recovery

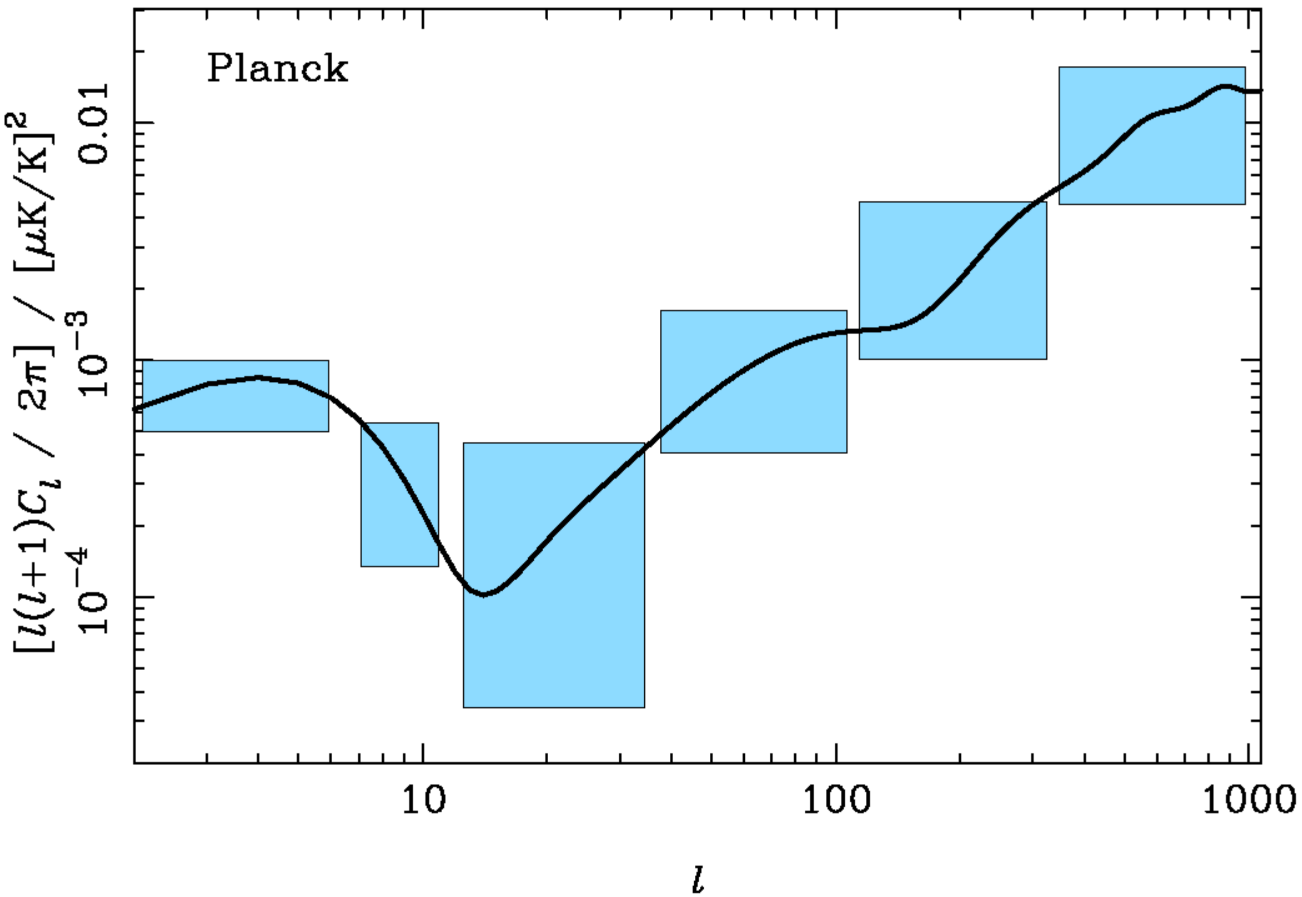

FIG 2.17.—Forecasts for the $\pm1\sigma$ errors on the B-mode polarization power spectrum C_ℓ^B from *Planck* (for $r = 0.1$ and $\tau = 0.17$). Above $\ell \sim 150$ the primary spectrum is swamped by weak gravitational lensing of the E-polarization produced by the dominant scalar perturbations. The cosmological model, and the assumptions about instrument characteristics, are the same as in Fig. 2.13.

From: Efstathiou 2004

PAPERS based on spherical wavelets

- Extragalactic point sources:
  - Cayón, et al., 2000 MNRAS 315, 757
  - Vielva, Martínez-González, Cayón, Diego, Sanz, Toffolatti, 2001, MNRAS, 326, 181
  - Vielva, Martínez-González, Gallegos, Toffolatti, Sanz, 2003, MNRAS, 344, 89
- Non-Gaussianity:
  - Martínez-González, Gallegos, Argüeso, Cayón, Sanz, 2002, MNRAS, 336, 22
  - Cayón, Sanz, Martínez-González, Banday, Argüeso, Gallegos, Gòrski, Hinshaw, 2001, MNRAS, 326, 1246
  - Cayón, Martínez-González, Argüeso, Banday, Gòrski, 2003, MNRAS, 339, 1189
  - Vielva, Martínez-González, Barreiro, Sanz, Cayón, 2004, ApJ, 609, 22
  - Cruz, Martínez-González, Vielva, Cayón, 2004, MNRAS, in press (astro-ph/0405341)
- Integrated Sachs-Wolfe Effect:
  - Vielva, Martínez-González, Tucci, 2004, MNRAS, submitted (astro-ph/0408252)

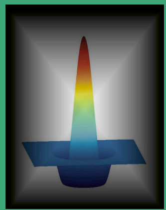

Wavelets

The wavelet transform provides us with information on:

- The scale of the structures present in the signal
- The position at which these structures are localized

It can be understood as a generalization of the Fourier transform.

$$w(R,\vec{b}) = \int d\vec{x}\, s(\vec{x})\Psi(\vec{x};R,\vec{b})$$

Continuous and rotationally invariant wavelet transform of a 2D signal.

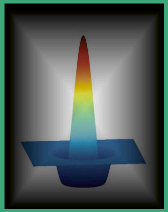

Wavelets

$$\boxed{\Psi(\vec{x};R,\vec{b})} = \frac{1}{\boxed{R}^2}\,\boxed{\psi\left(\frac{\left|\vec{x}-\vec{b}\right|}{R}\right)}$$

Wavelet at scale *R* and position $\vec{b}$

Scale

Mother wavelet

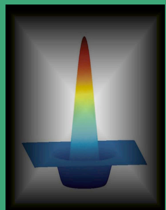

Wavelets

The mother wavelet satisfies:

Efective filter

$$\boxed{\int d\vec{x}\,\psi = 0,} \qquad \text{compensation}$$

$$\int d\vec{x}\,\psi^2 = 1, \qquad \text{normalization}$$

$$C_\psi = (2\pi)^2 \int dk\,k^{-1}\hat{\psi}^2(k) < \infty, \qquad \text{admisibility}$$

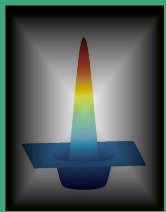

The Mexican Hat Wavelet (Marr)

The simplest wavelet is the Mexican Hat Wavelet (MHW). It is the Laplacian of a Gaussian.

$$\psi(x) \propto -\Delta e^{-(x^2/2R^2)} \equiv \frac{1}{\sqrt{2\pi}}\left[2-\left(\frac{x}{R}\right)^2\right]e^{-\frac{x^2}{2R^2}}$$

$$\hat{\psi}(k) \propto (kR)^2 e^{-\frac{1}{2}(kR)^2}$$

The Spherical Mexican Hat Wavelet

The extension of the Euclidean MHW to the sphere is made by a stereografic proyection of the MHW to the tangential plane (Antoine & Vanderheynst 1998).

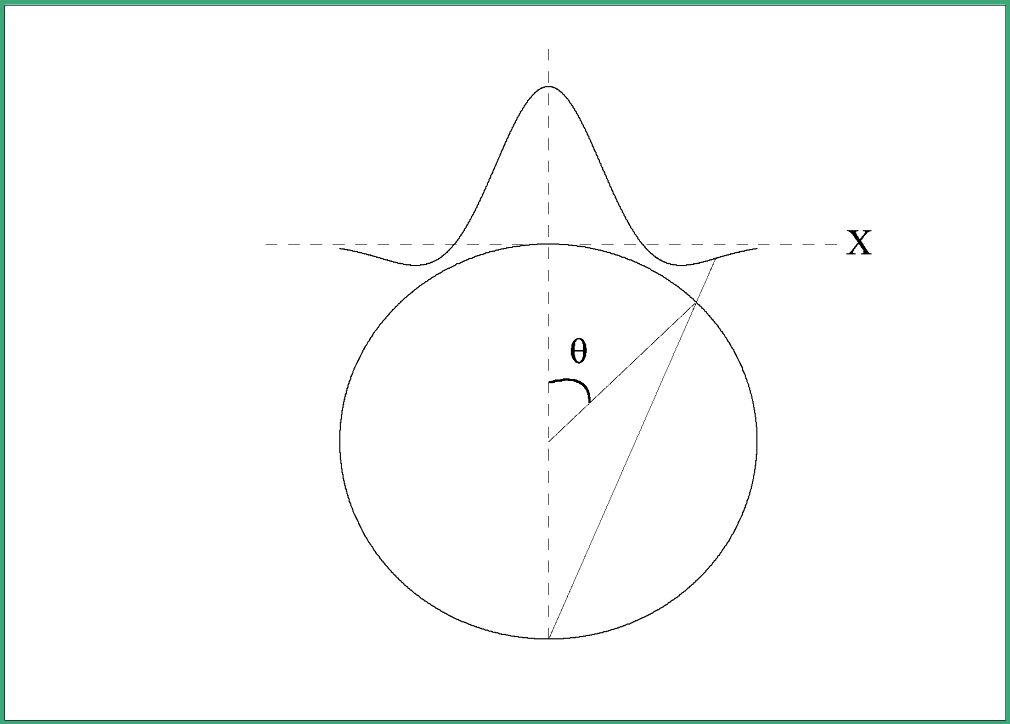

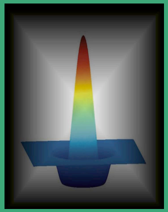

The Spherical Mexican Hat Wavelet

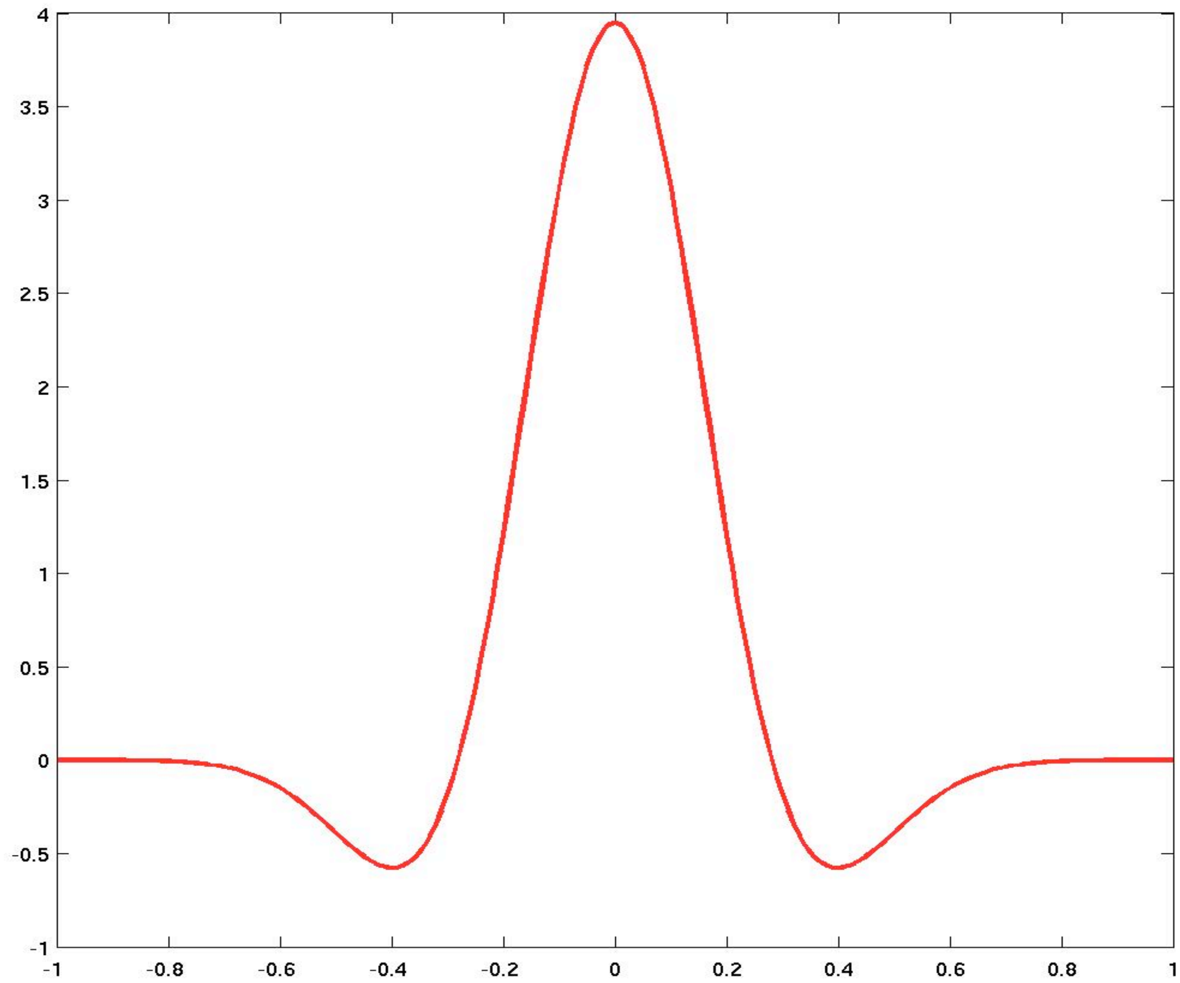

SMHW in 2D

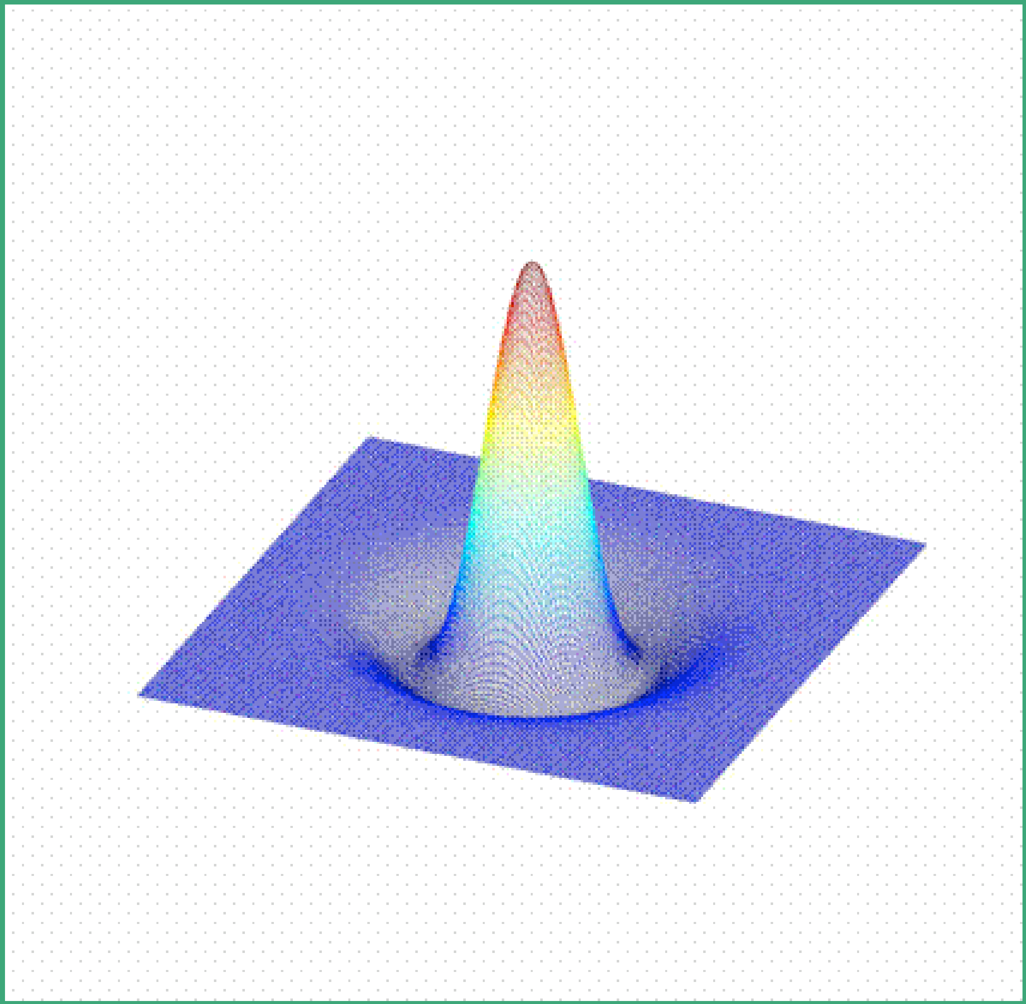

DETECTION OF EXTRAGALACTIC POINT SOURCES

- Extragalactic point sources are interested to study: as galaxy populations of different types and also to remove them from CMB.
- They have the shape of the antenna response which is aproximately Gaussian.
- Then the amplitude of the source relative to the background is amplified after convolving with the MHW at the appropriate scale.
- Usual methods to detect stars or galaxies in optical data (like SEXTRACTOR) do not work in microwave images. The reason is that in the later the background is much stronger showing a wild behaviour.
- The method based on the MHW is tested with “realistic” simulations of the Planck mission.
- The method has been also tested with real data (SCUBA) and is now been applied to the WMAP data.

DETECTION OF POINT SOURCES

$$s(\vec{x}) \equiv s(x) = \frac{I}{2\pi\sigma_a^{2}} e^{-\frac{x^2}{2\sigma_a^{2}}}$$

Point source

The MHW coeficient in the position of the maximum is given by:

$$w(R) = 2\sqrt{2\pi}\, I R \frac{\left(R/\sigma_a\right)^2}{\left(1 + \left(R/\sigma_a\right)^2\right)^2}$$

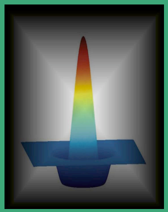

DETECTION OF POINT SOURCES

The point sources are amplified in wavelet space:

$$A(R) = \frac{w(R)/\boxed{\sigma_w(R)}}{I/\boxed{\sigma_m}}$$

Map dispersion

$$\sigma_w^{\,2}(R) \propto \int dk\, k\, P(k) \left|\Psi(k)\right|^2$$

DETECTION OF POINT SOURCES

An optimal scale given by the data can be found:

$$R_o = f\left(P(k), \sigma_a\right)$$

DETECTION OF POINT SOURCES

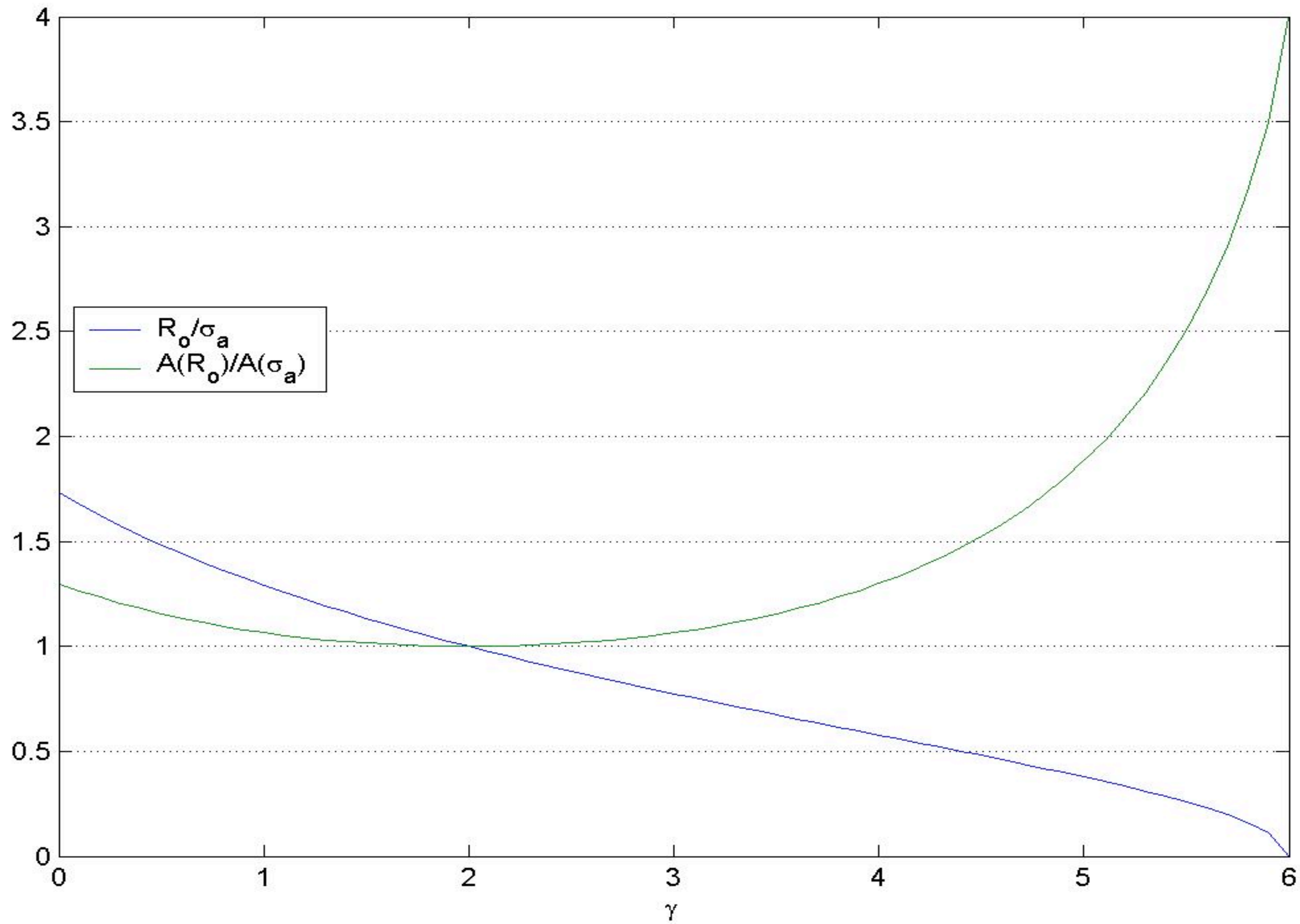

The MHW versus the MF

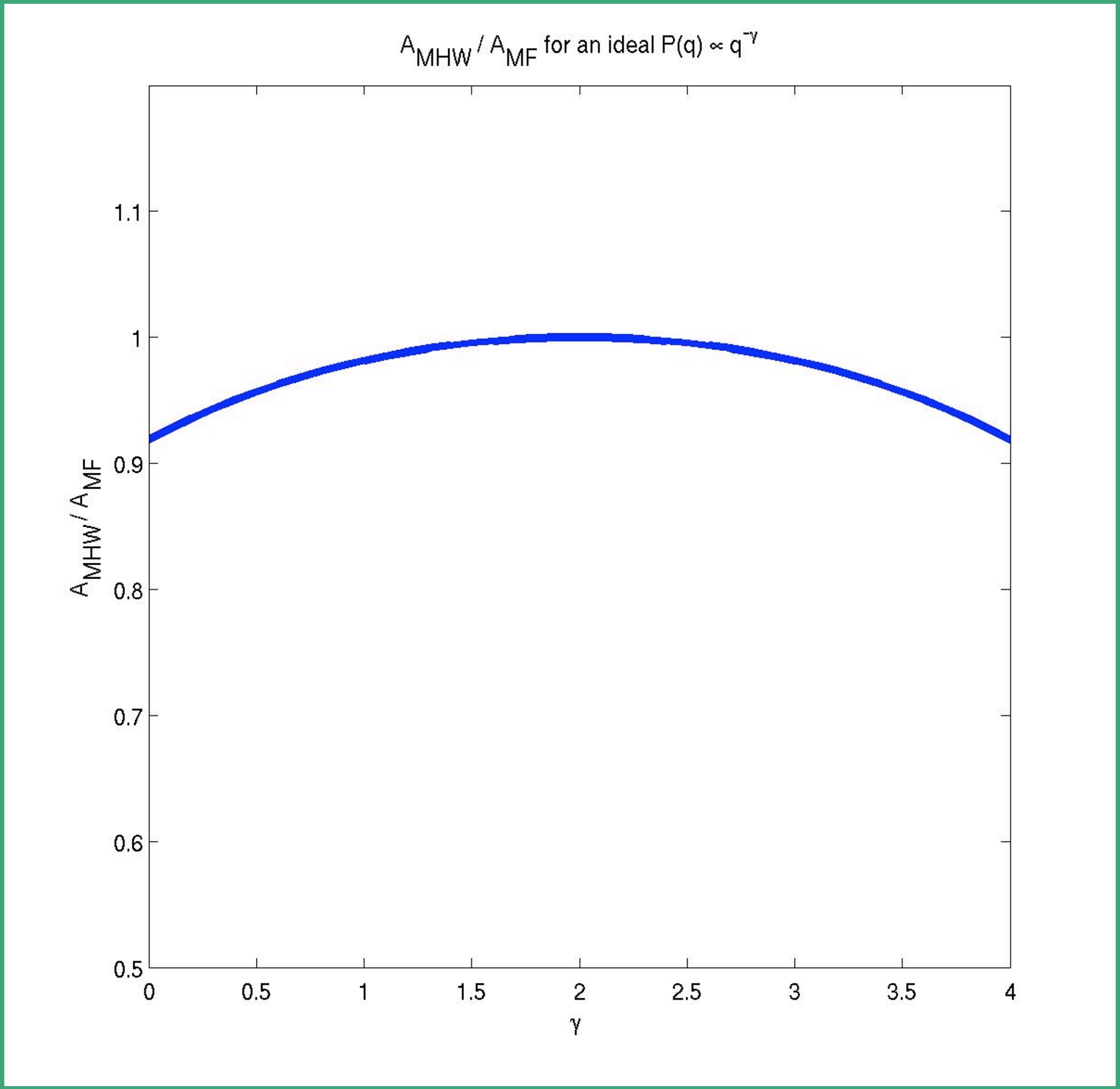

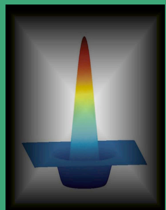

DETECTION OF POINT SOURCES

The source amplitude is estimated by a multiscale fit (the optimal scale + 3 adyacents).

$$\chi_l^2 = \sum_{i,j} \left(w(R_i,\vec{b}_l)^t - w(R_i,\vec{b}_l)^e \right) V_{ij}^{-1} \left(w(R_j,\vec{b}_l)^t - w(R_j,\vec{b}_l)^e \right)$$

$$V_{ij} = \frac{1}{N} \sum_{l=1}^{N_{pix}} w(R_i,\vec{b}_l)^e \, w(R_j,\vec{b}_l)^e$$

The MHW: Euclidean application

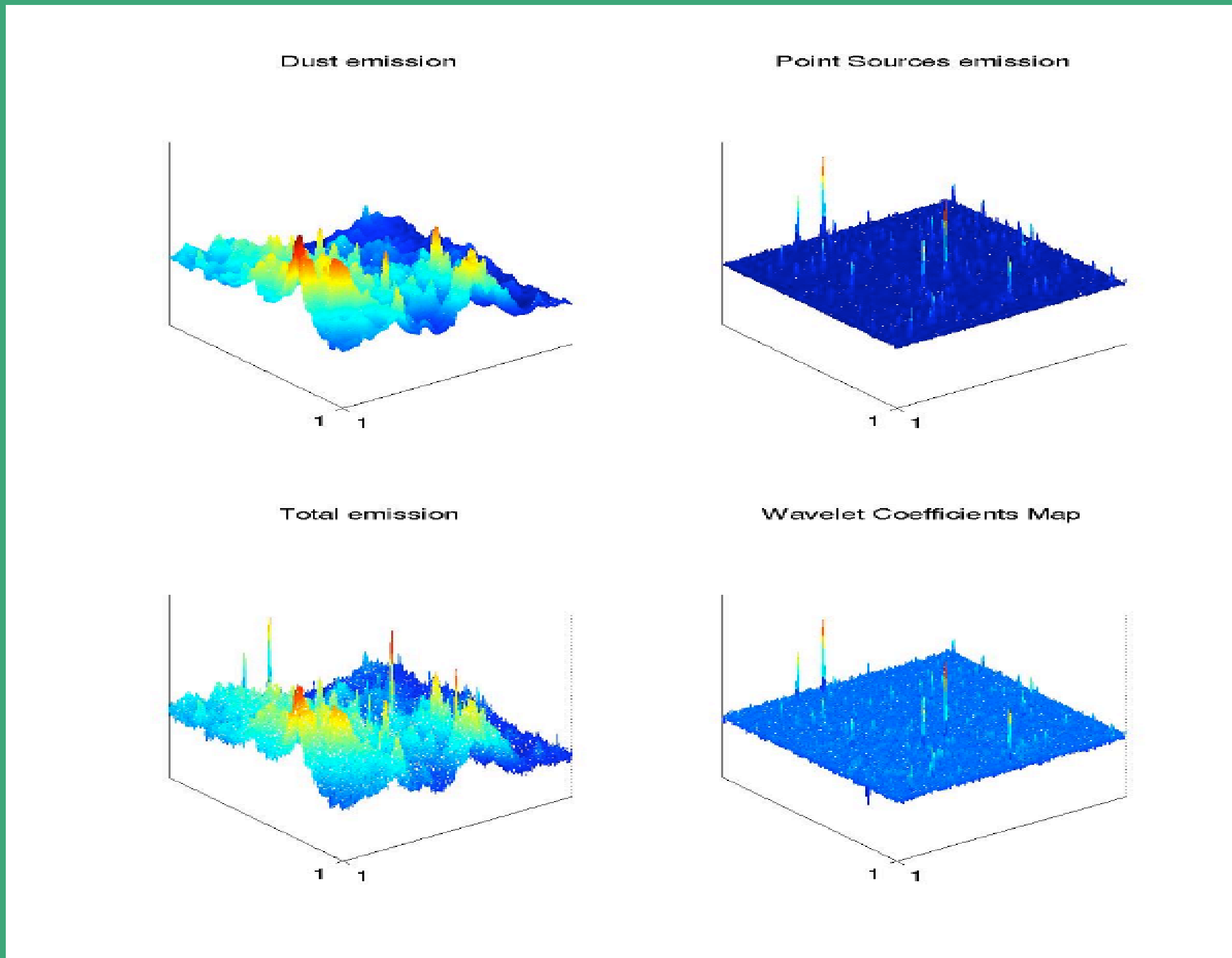

The MHW: Spherical application

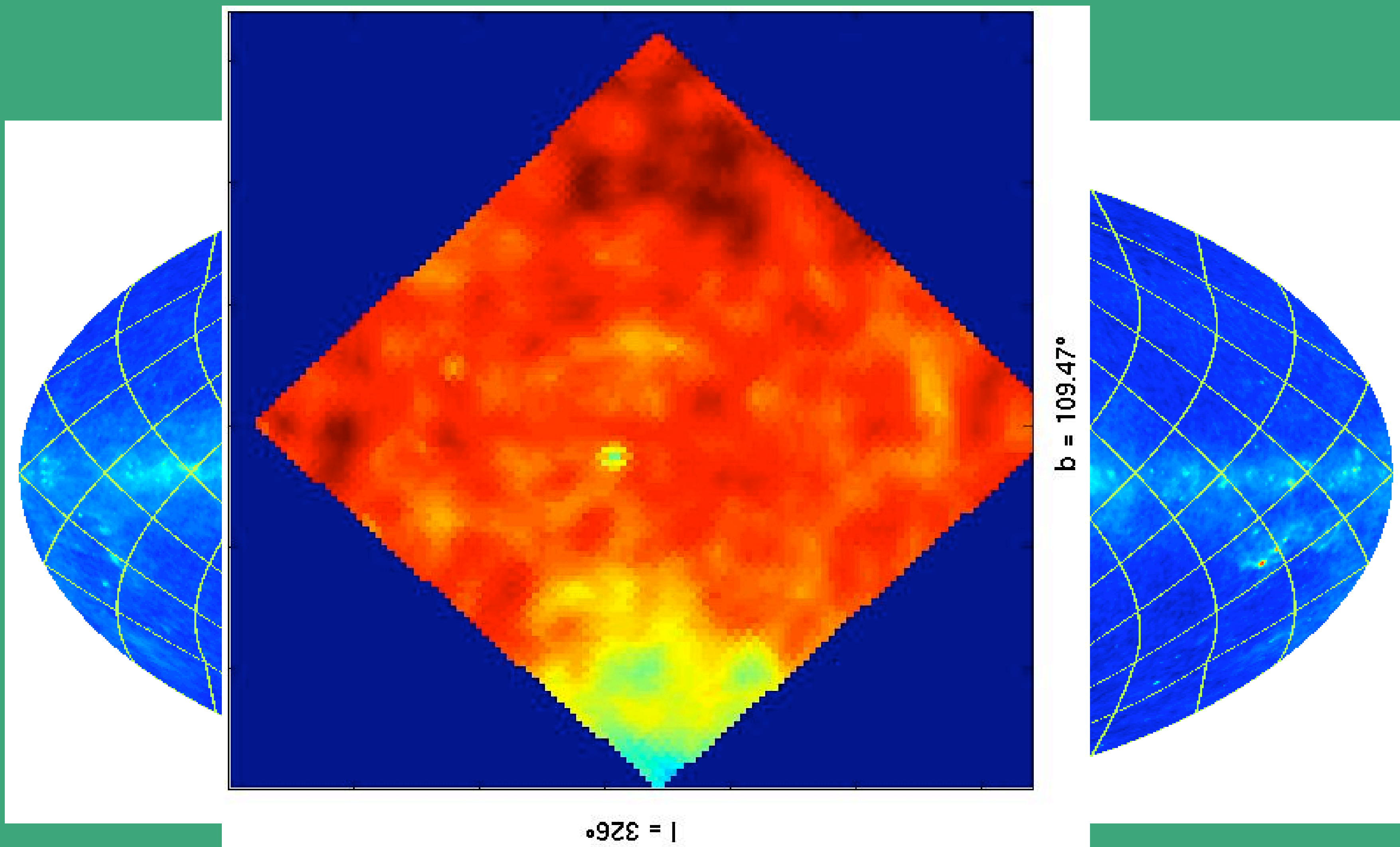

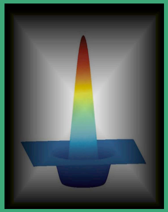

The MHW: Spherical application

Point sources detected at 30 GHz

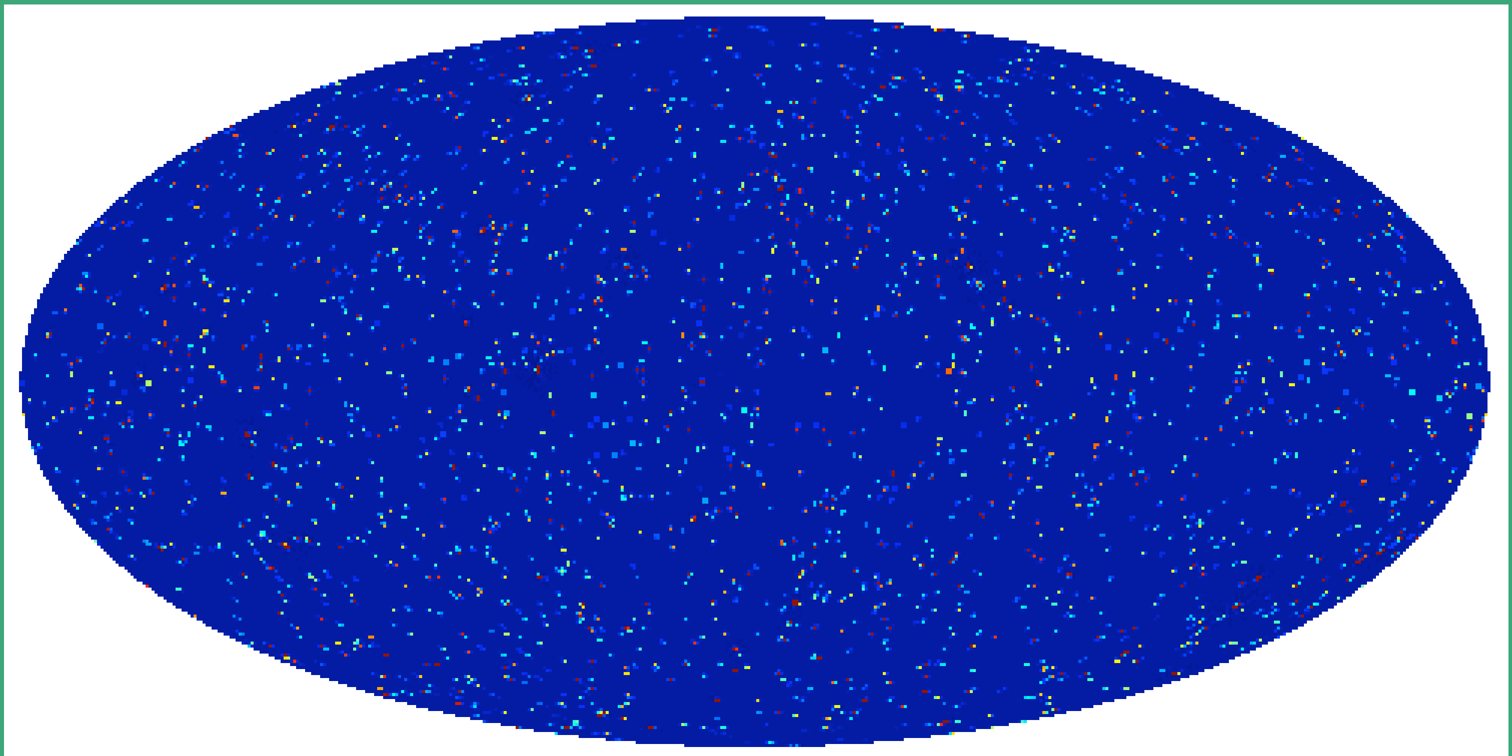

Extragalactic source catalogue – Planck mision

Freq.	#	Jy	Error (%)	Bias (%)	Cut (º)	N_{op}	Comp(%)
857	27257	0.48	17.7	-4.4	25	17	70
545	5201	0.49	18.7	4.0	15	15	75
353	4195	0.18	17.7	1.4	10	10	70
217	2935	0.12	17.0	-2.5	7.5	4	80
143	3444	0.13	17.5	-4.3	2.5	2	90
100	3342	0.16	16.3	-7.0	0	4	85
70	2172	0.24	17.1	-6.7	0	6	80
44	1987	0.25	16.4	-6.4	0	9	85
30	2907	0.21	18.7	1.2	0	7	85

See also applications of the method to real data: SCUBA (Barnard et al. 2004, MNRAS, 352, 961), WMAP (Cruz et al. 2004, in preparation)

NON-GAUSSIANITY

- Why a Gaussian analysis?:
  - Standard model of inflation predicts Gaussian temperature fluctuations, however non-standard inflation or topological defects predict deviations from Gaussianity in different ways.
  - Secondary anisotropies (like reionization, Rees-Sciama effect or gravitational lensing) generate non-Gaussian fluctuations.
  - The standard approach to estimate the cosmological parameters assumes that the CMB signal is Gaussian.
  - Gaussianity analyses are needed to check for systematics in the data.

NON-GAUSSIANITY ANALYSIS OF WMAP DATA

- WMAP team finds consistency with Gaussianity using the bispectrum and the Minkowski functionals (Komatsu et al. 2003).
- Later several groups have found asymmetries or non-Gaussian signatures in the WMAP data (Park 2004, Eriksen et al. 2004a,b, Vielva et al. 2004, Mukherjee and Wang 2004, Cruz et al. 2004, Hansen et al. 2004a,b, Larson and Wandelt 2004, Mcewen et al. 2004)
- Hypotheses:
    - The CMB is a homogeneous and istropic random field on the sphere
    - The CMB is a multivariate Gaussian R. F. (or equivalently the a_{lm} are Gaussian)
    - The receiver beam responses are well characterised by the WMAP team and the anisotropic noise is uncorrelated and its amplitud well estimated
    - The WMAP data are free from systematics
    - The WMAP data outside the kp0 mask are not contaminated by foregrounds
    - The uncertainties in the cosmological parameters have a negligible effect on the results

The data: co-added Q-V-W WMAP

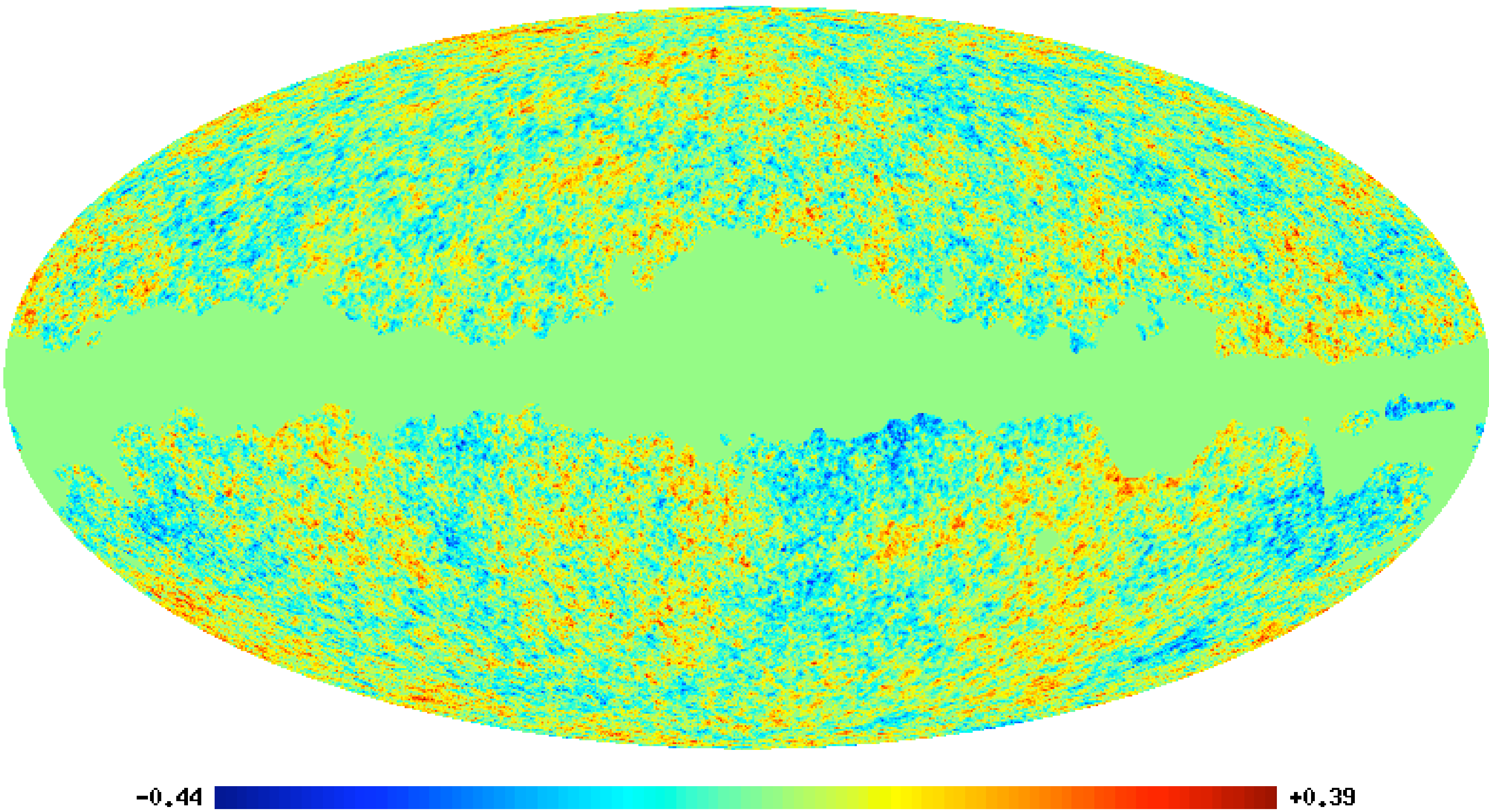

The Spherical Mexican Hat Wavelet (SMHW)

Skewn

$S(R)$ =

$^4 - 3$

N

$)$

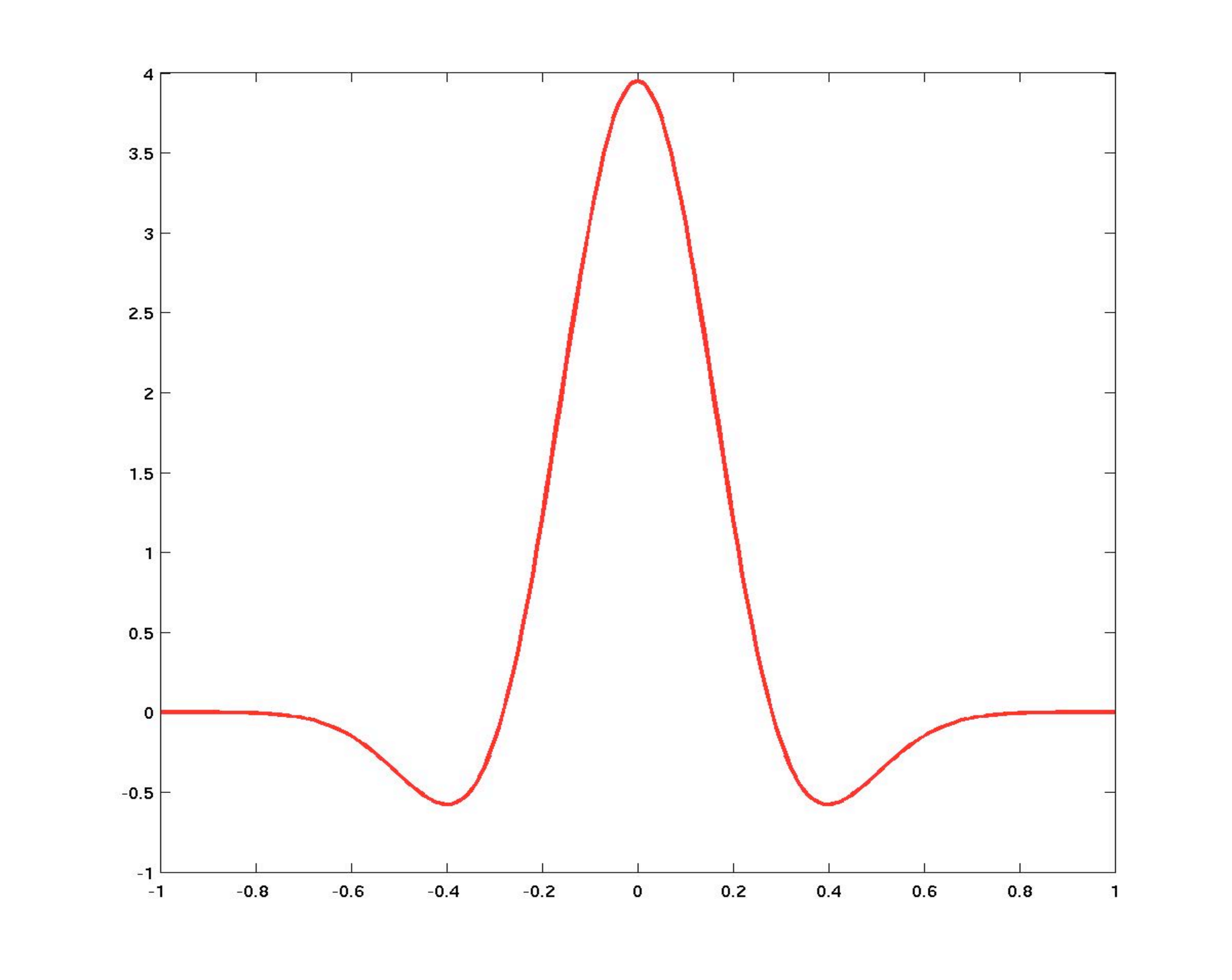

Creating the *exclusion masks*

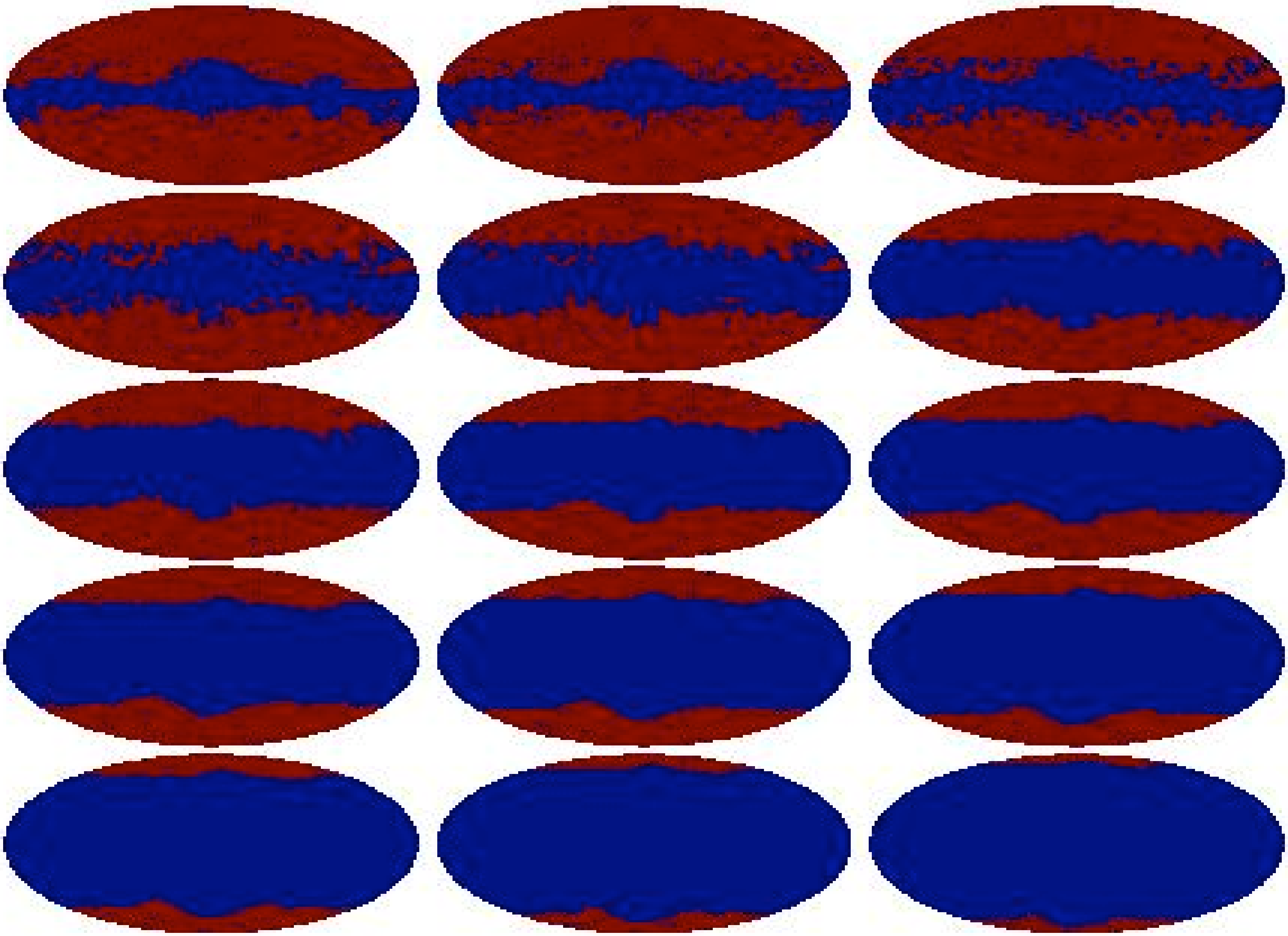

SMHW SCALES

R: 1: 13.7, 2: 25, 3: 50, 4: 75, 5: 100, 6: 150, 7: 200, 8: 250, 9: 300, 10: 400, 11: 500, 12: 600, 13: 750, 14: 900, 15: 1050

THE RESULTS

SMHW coefficient map at R_8 = 250 arcmin   above 3_

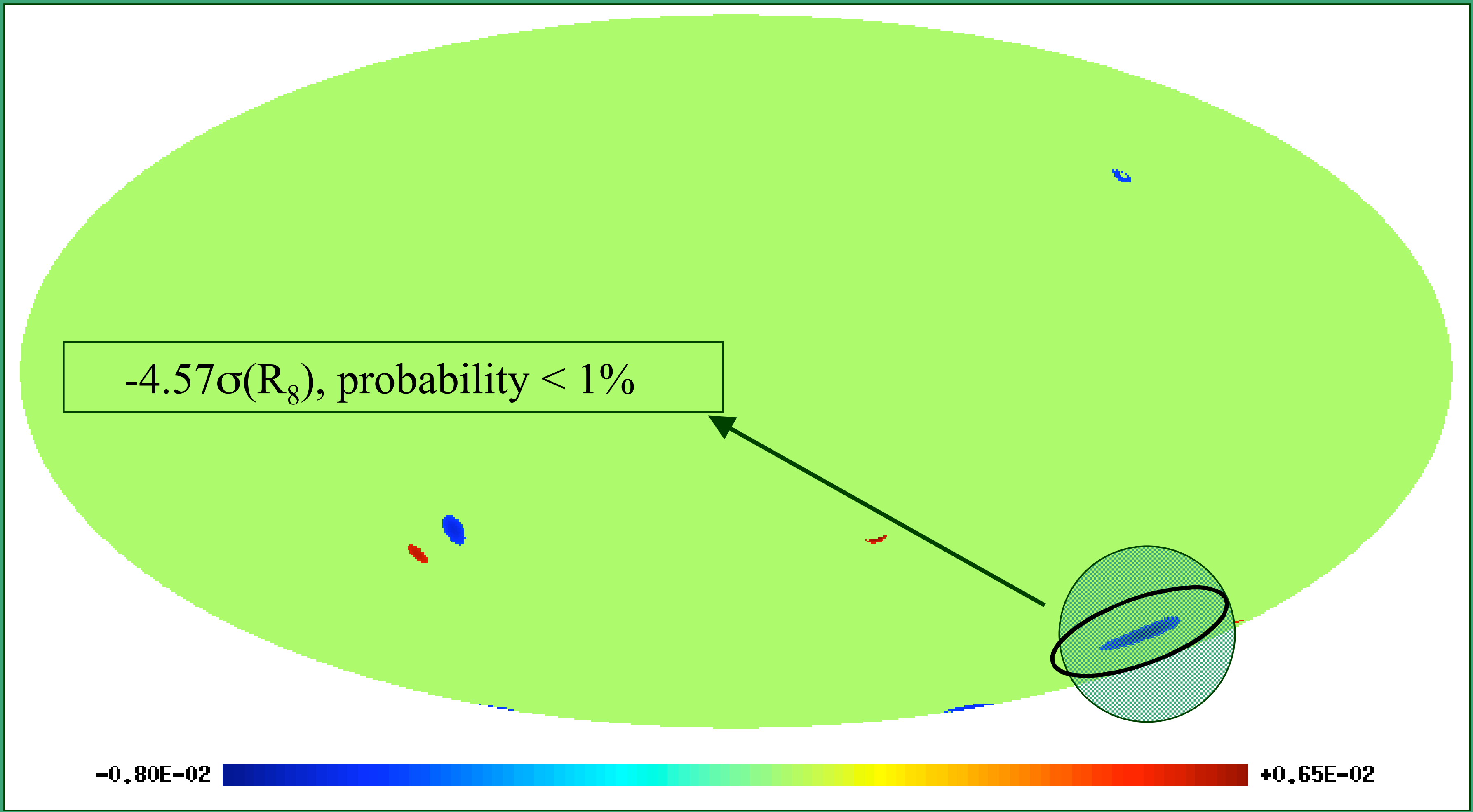

Vielva et al. 2004

Is it due to systematics? (1)

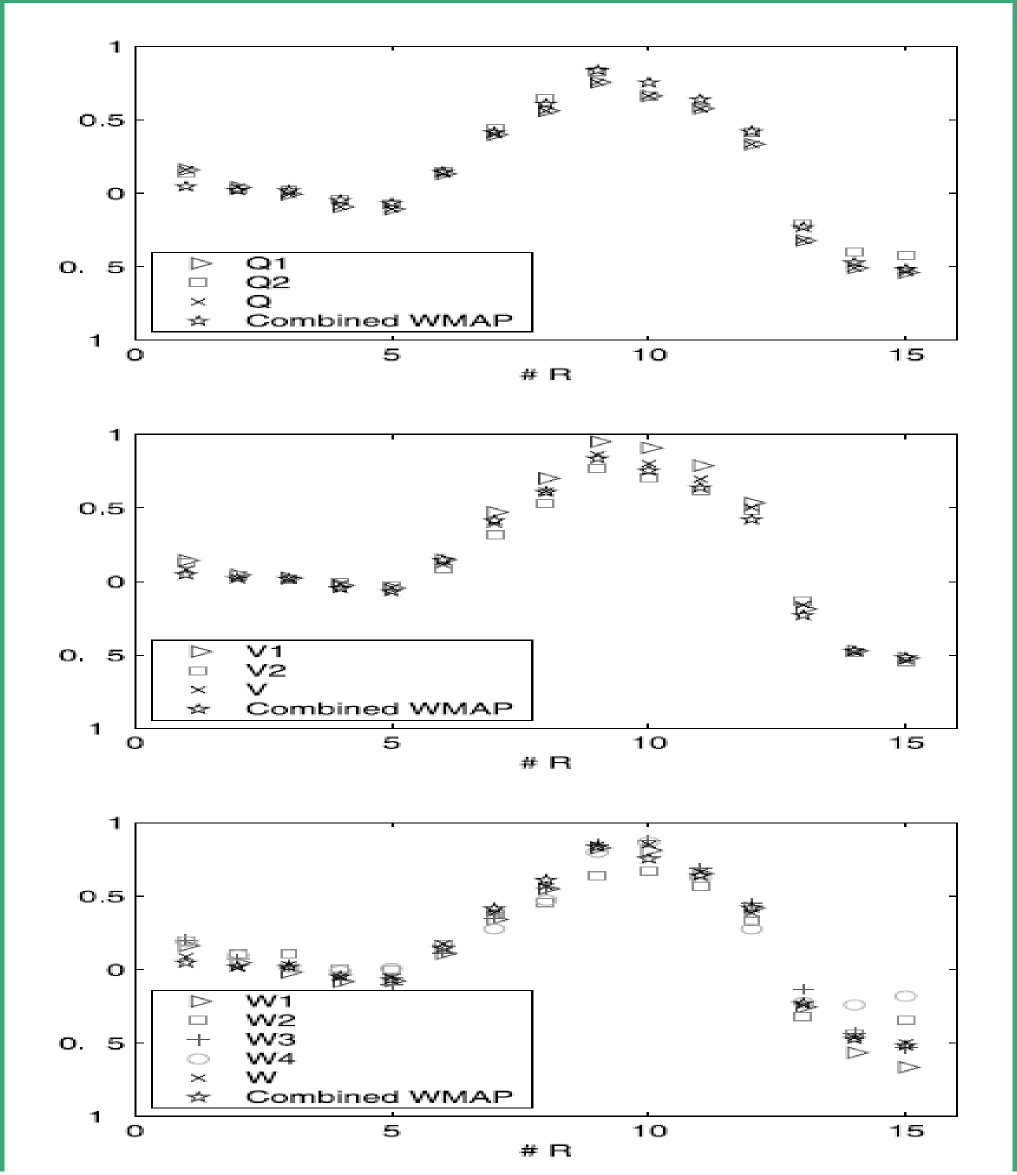

Is it due to systematics? (2)

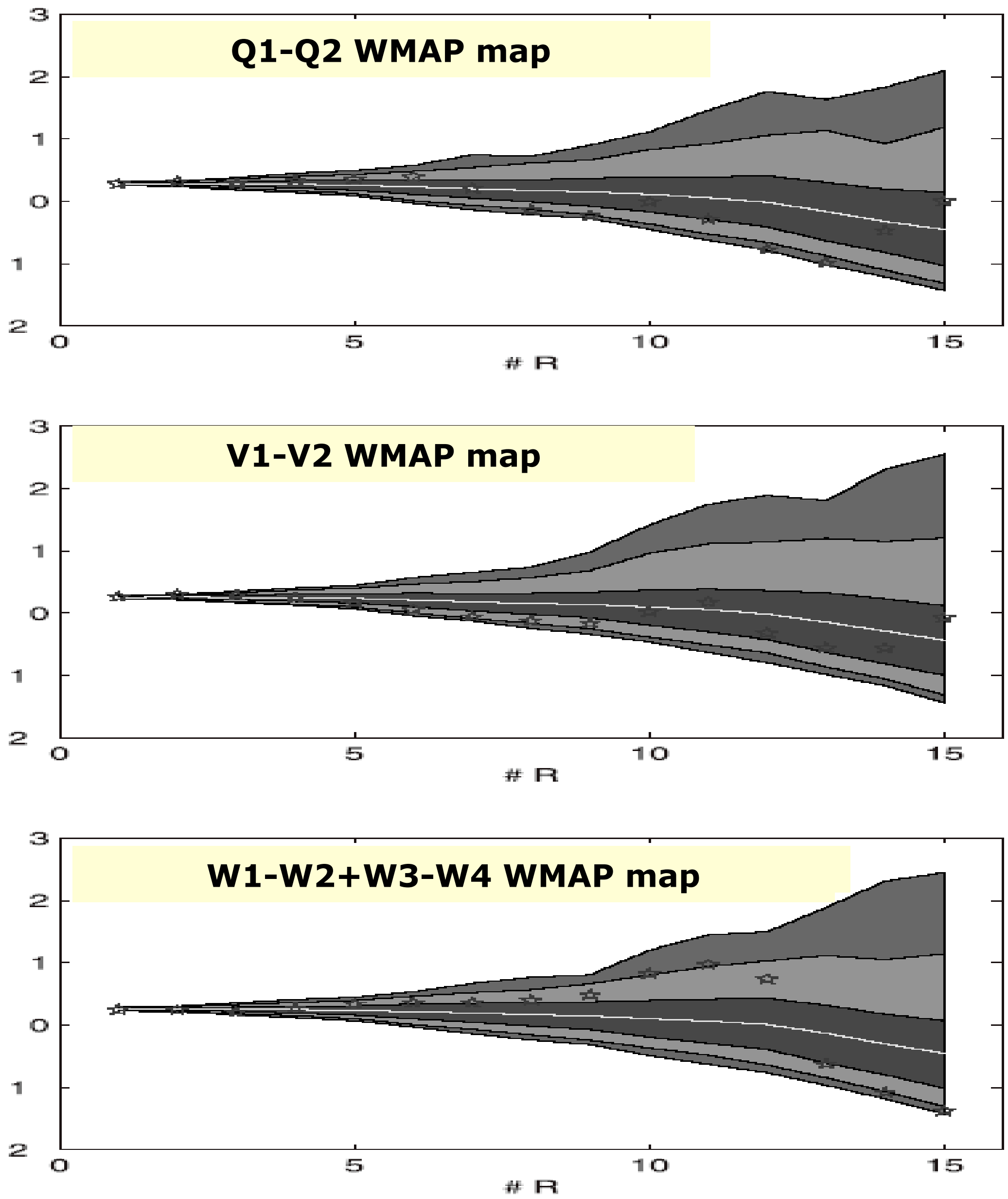

Is it due to systematics? (3)

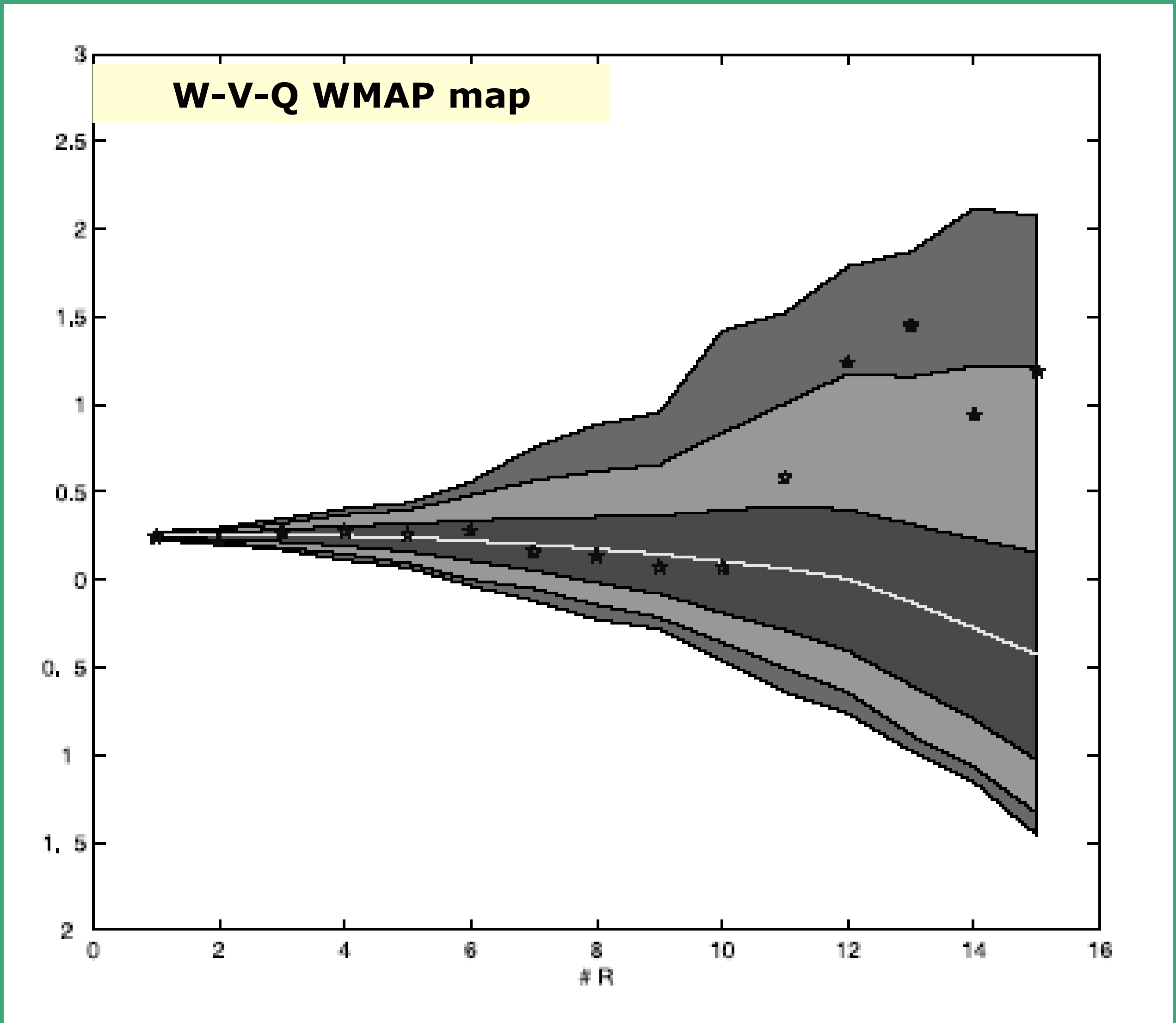

Is it due to systematics? (4)

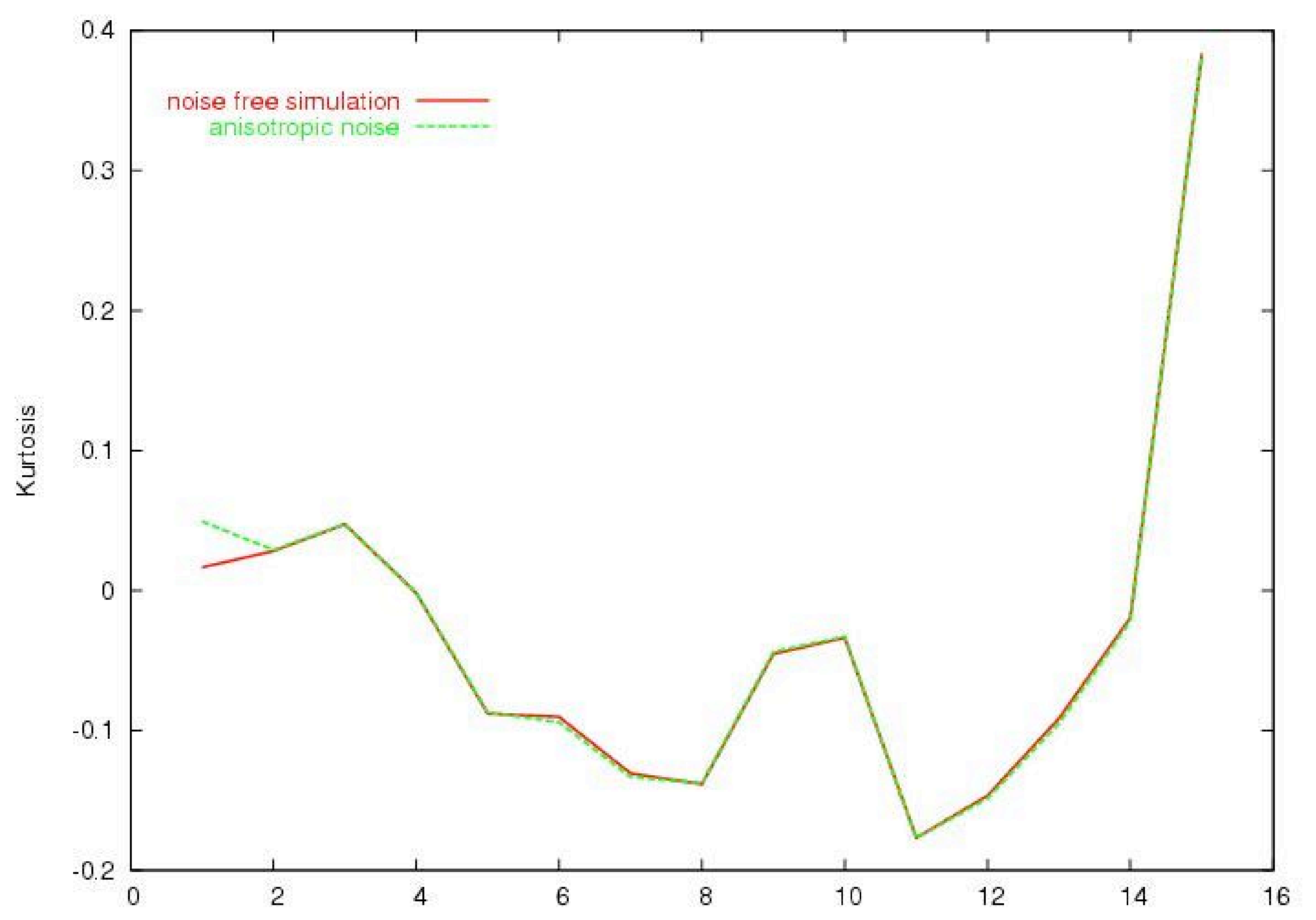

Is it due to systematics? (5)

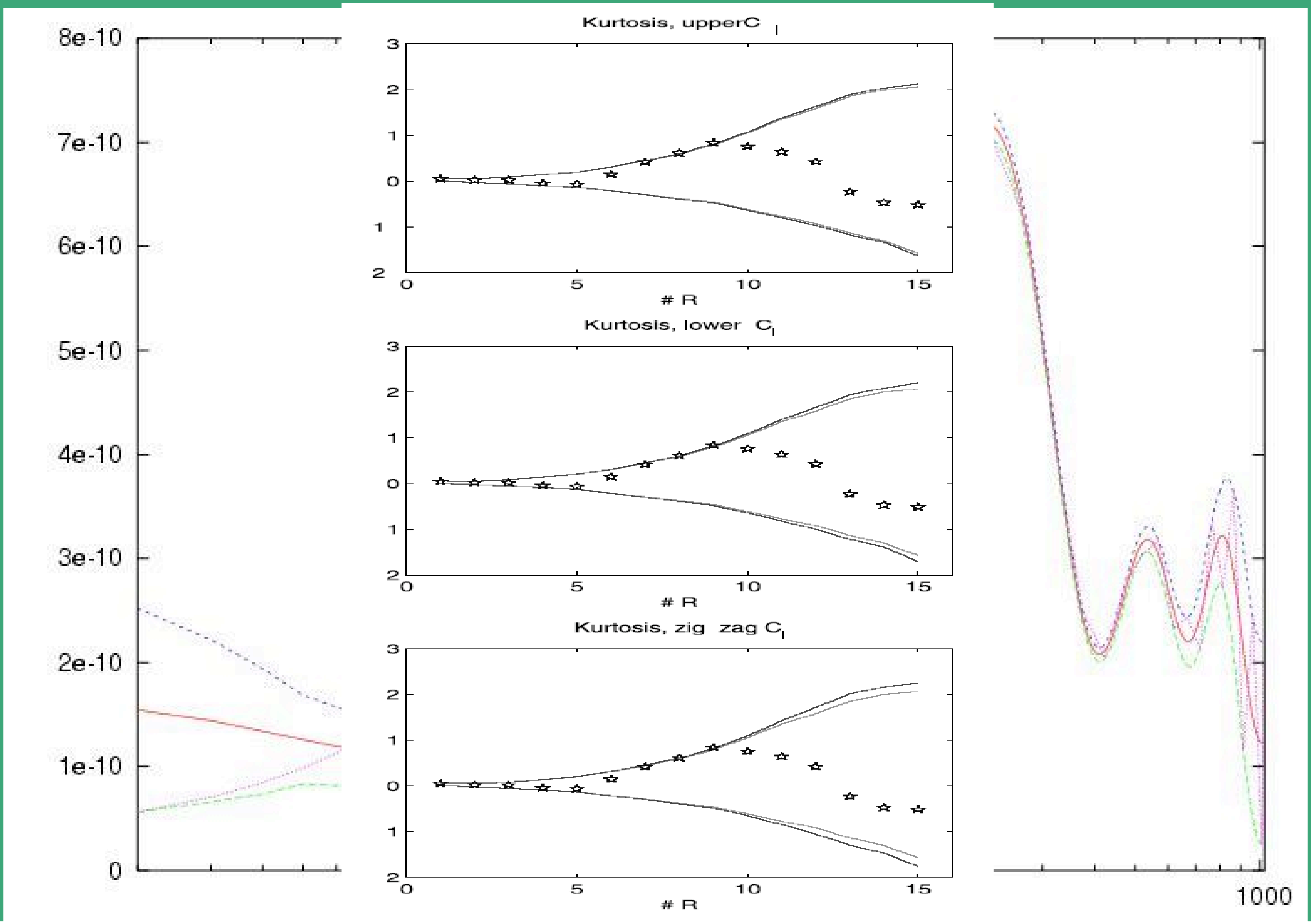

Is it due to systematics? (6)

Whitening of the data

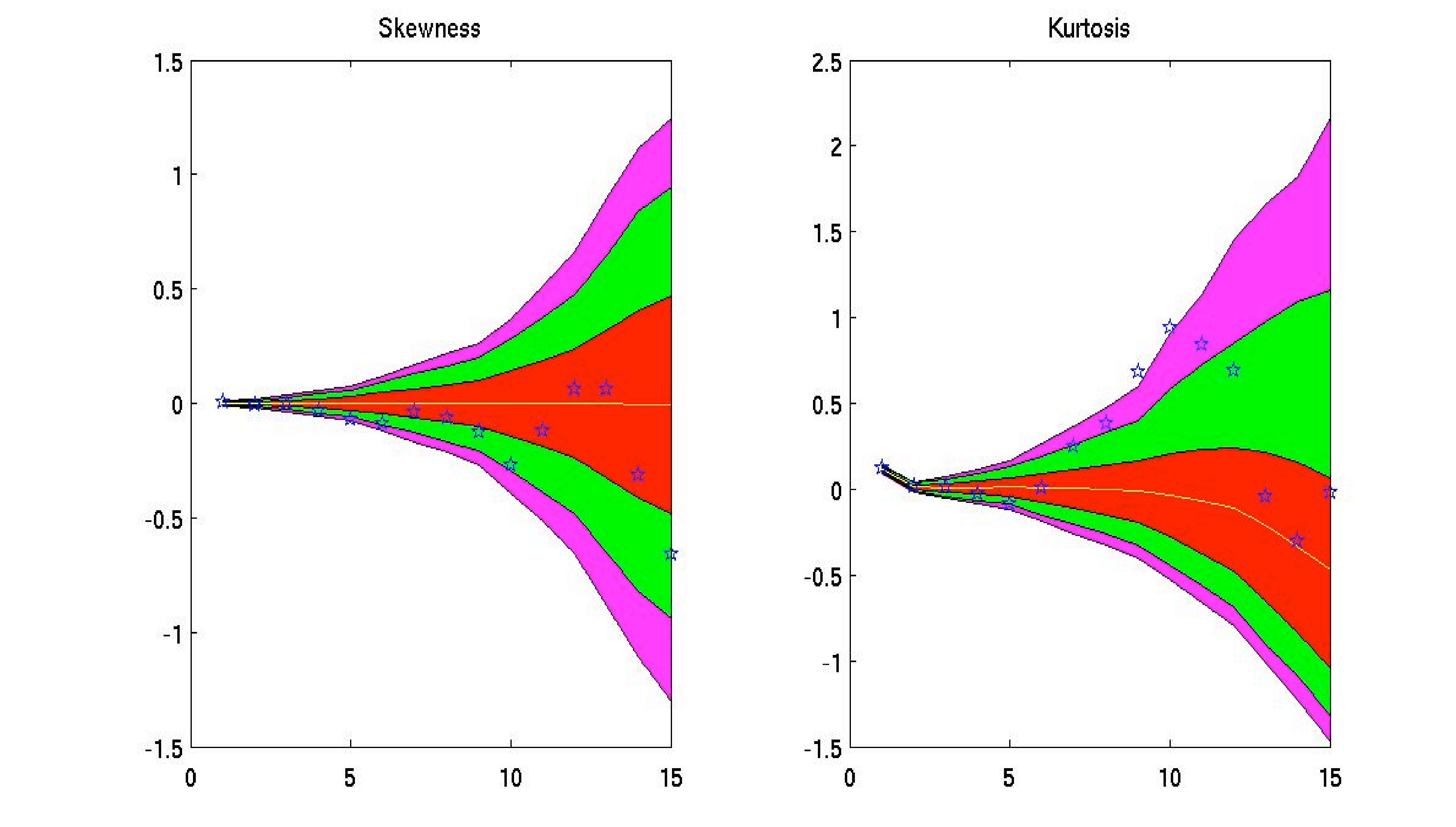

Is it due to foregrounds? (1)

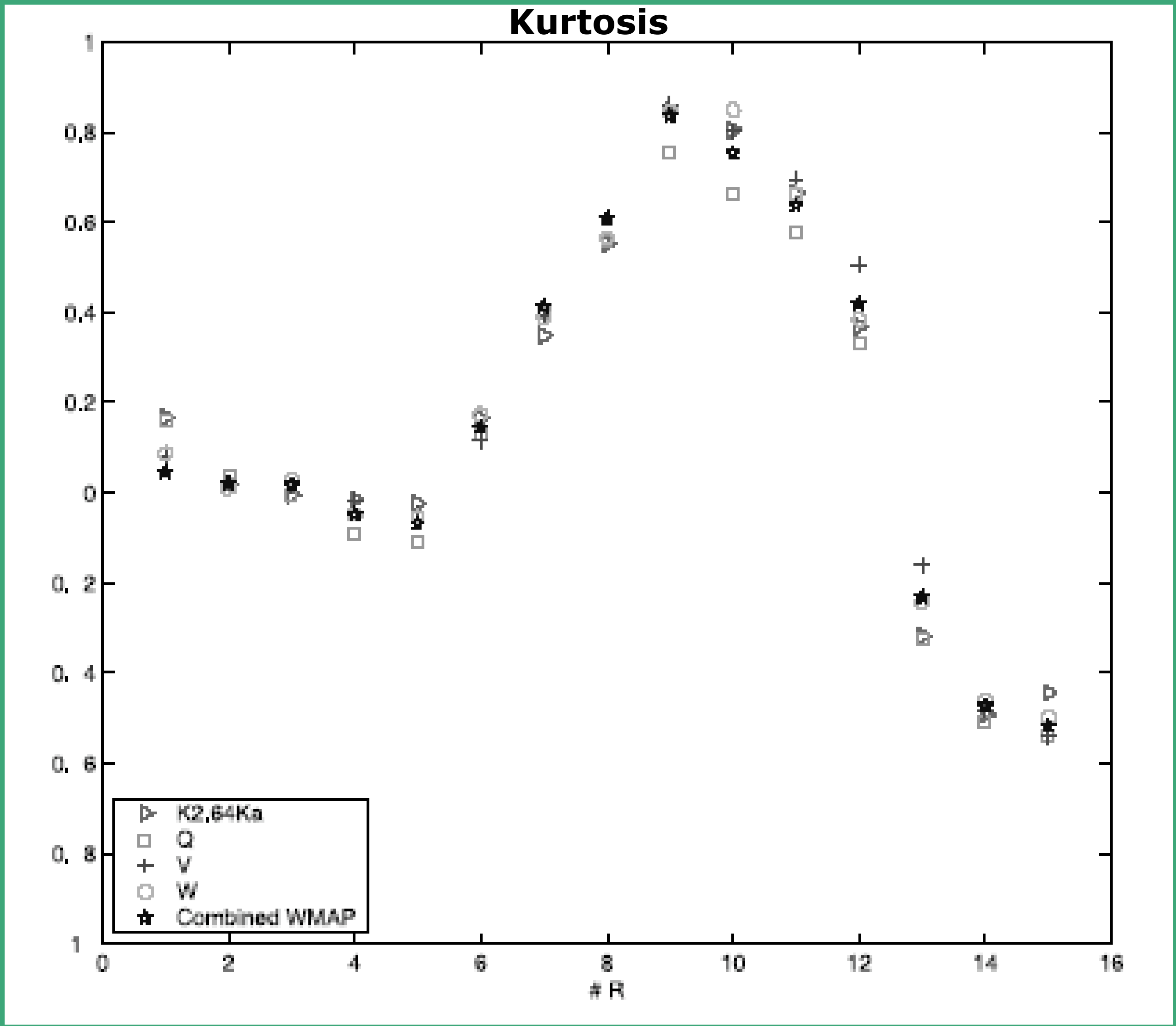

Is it due to foregrounds? (2)

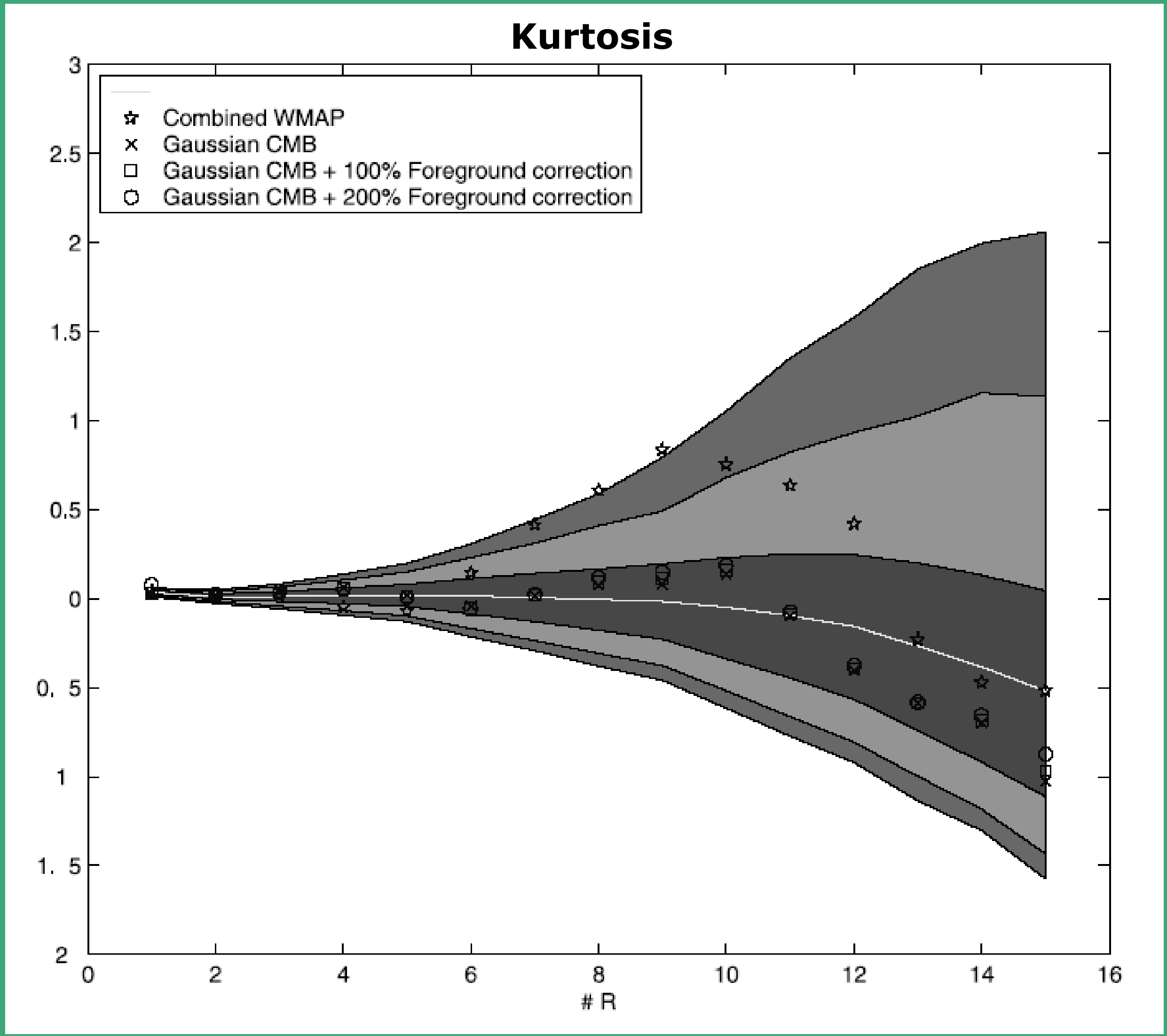

Is the Spot alone the cause of the Non-Gaussianity?

Histogram of the biggest cold spot

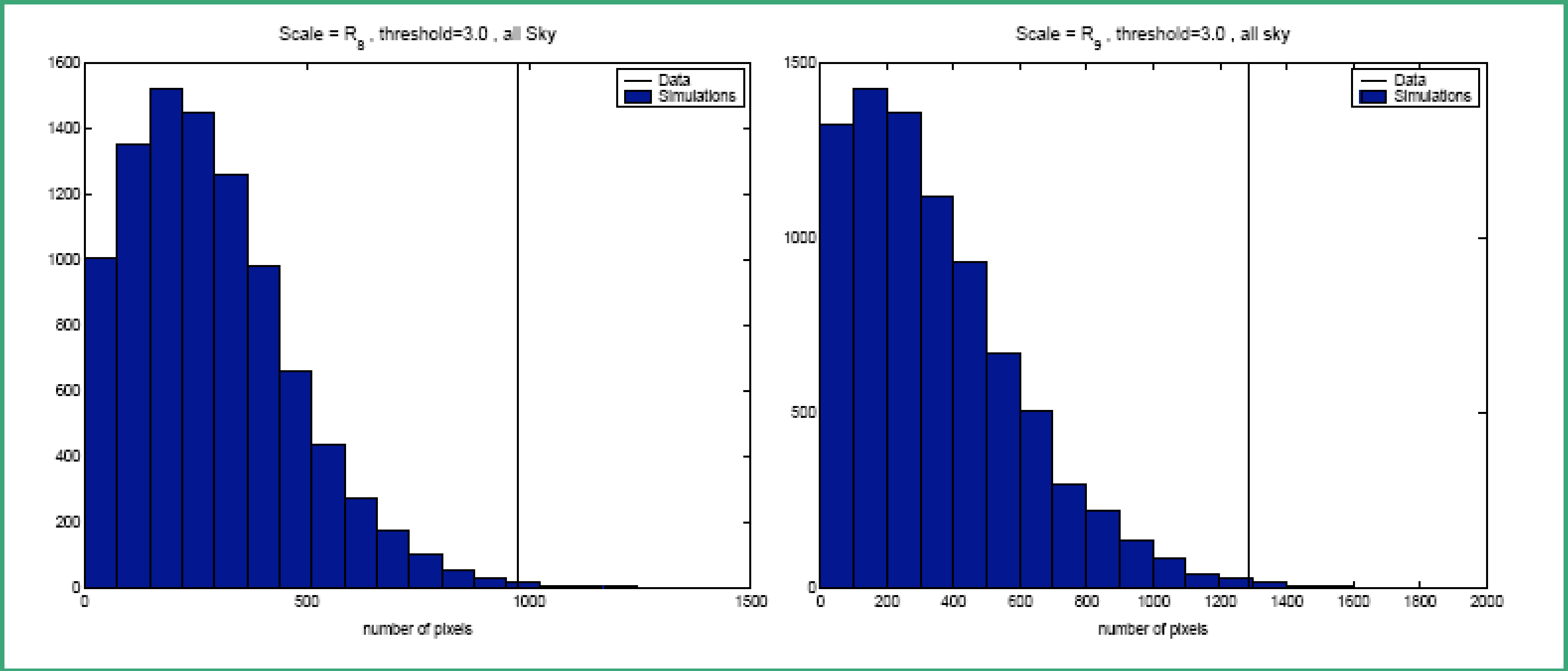

Cruz et al. 2004, astro-ph/0405341

Scale	threshold	probability
R_8	3.0	0.34%
	3.5	0.32%
	4.0	0.41%
	4.5	0.65%
R_9	3.0	0.38%
	3.5	0.21%
	4.0	0.18%
	4.5	0.22%

Is the Spot alone the cause of the Non-Gaussianity?

Histogram of the total cold area

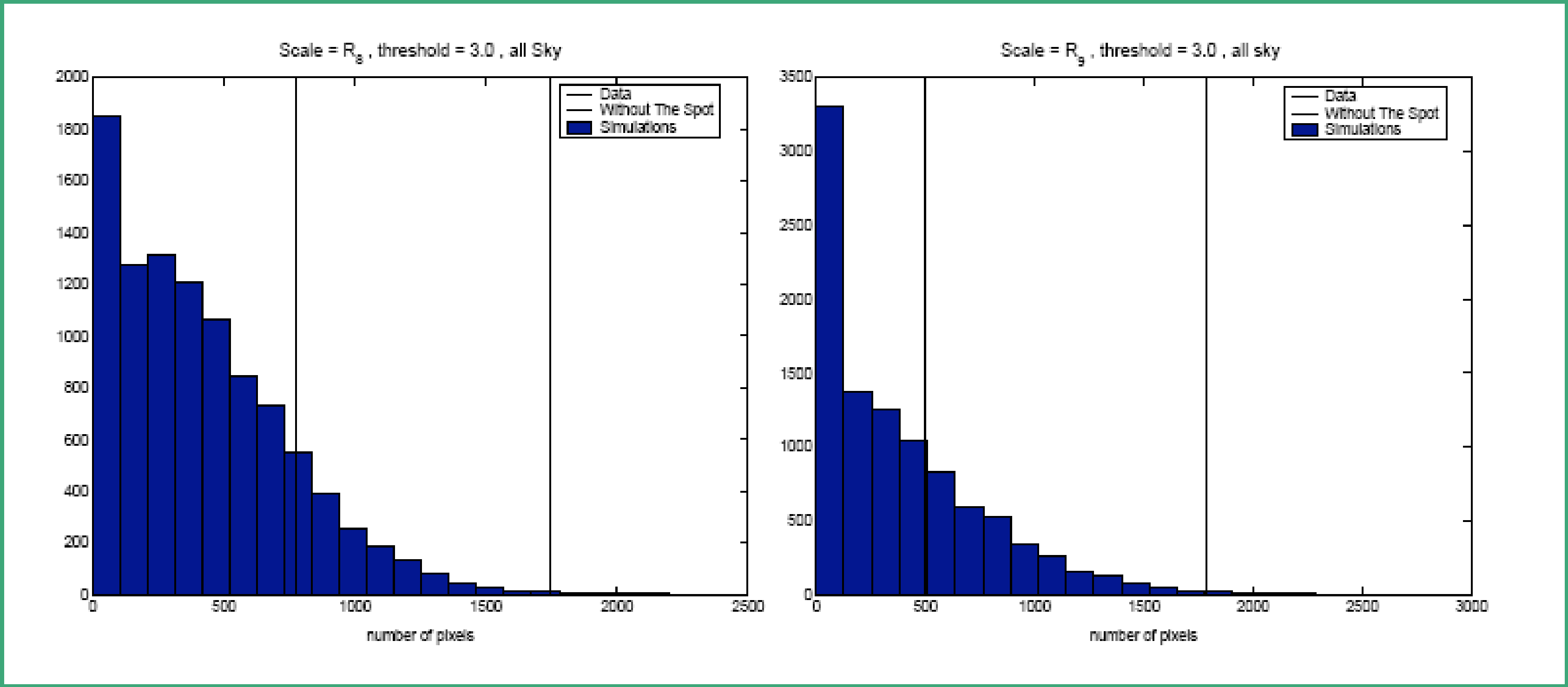

Cruz et al 2004, astro-ph/0405345

Scale	threshold	P with Spot	P without Spot
R_8	3.0	0.18%	14.79%
	3.5	0.28%	18.28%
	4.0	0.45%	-
	4.5	0.65%	-
R_9	3.0	0.39%	30.53%
	3.5	0.18%	17.68%
	4.0	0.19%	-
	4.5	0.22%	-

Is the Spot the only cause of Non-Gaussianity?

All Spot pixels above 3σ masked

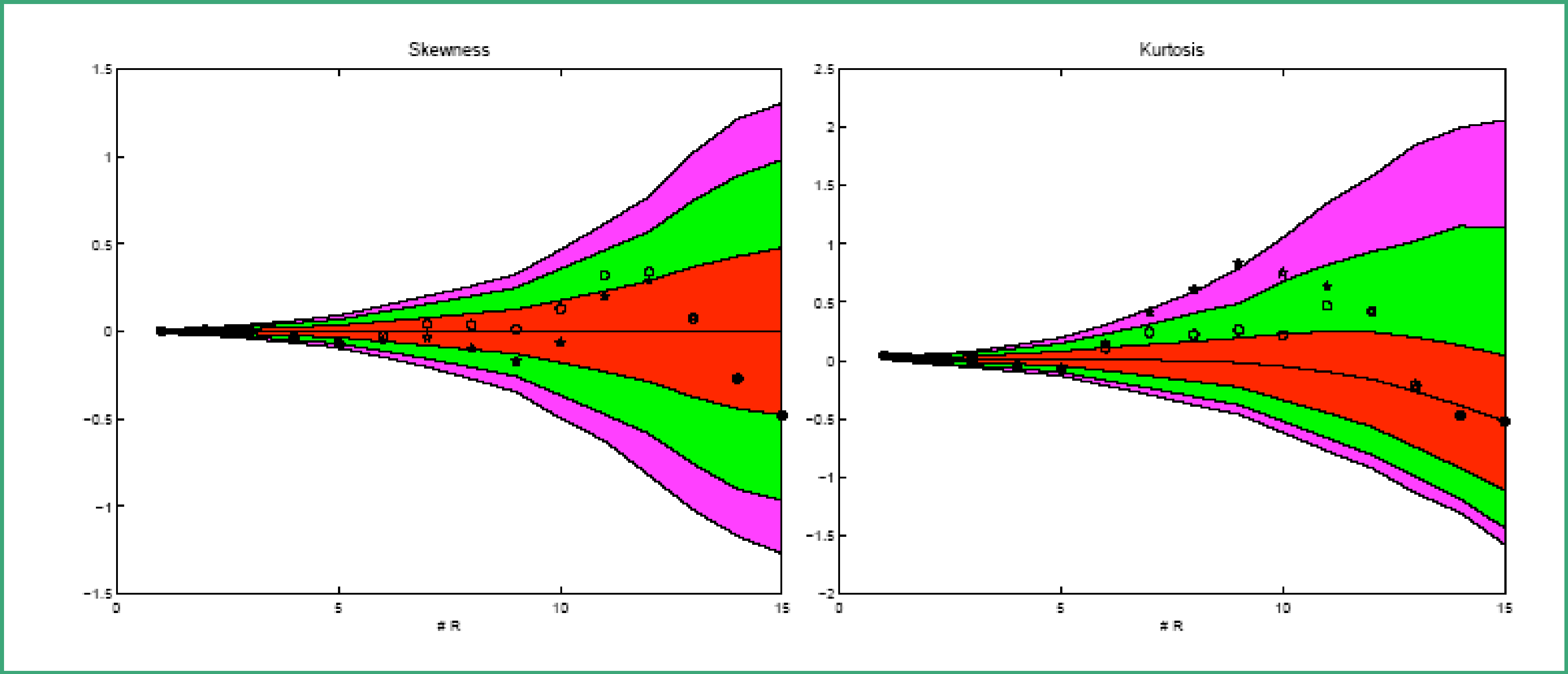

So... is it due to intrinsic fluctuations?

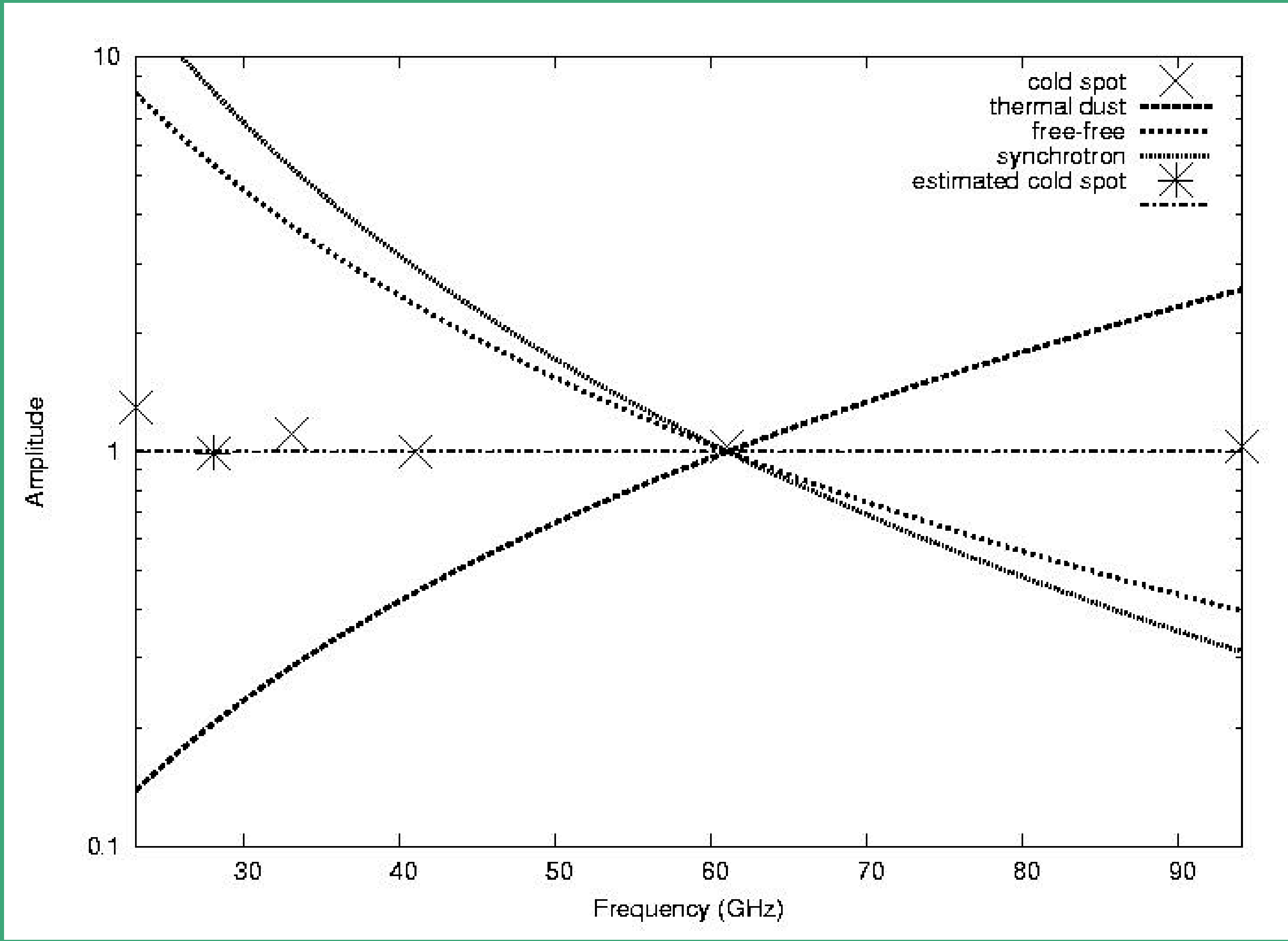

Conclusions of non-Gaussianity analysis

- A non-Gaussian feature has been detected at >99.6% c.l. in the kurtosis of the SMHW coefficients at R around 4 degrees.
- The excess kurtosis is caused by a single large cold Spot placed at (b=-57°, l=209°). Its probability is <0.2%.
- Systematic effects (like beams and noise) do not seem to generate this non-Gaussianity.
- Galactic foregrounds, point sources and SZ effect due to galaxy clusters seem not to generate the NG signal.
- Intrinsic fluctuations (both secondary anisotropies and primordial seeds) can not be rejected.

THE ISW EFFECT

- The Integrated Sachs-Wolfe (ISW) effect (Sachs-Wolfe 1967) is due to the gravitational redshift suffered by the CMB photons when crossing the time-varying gravitational potentials of the LSS.
- In the Einstein-de Sitter model the ISW effect is zero. Thus a positive detection of the effect implies the existence of dark energy in the case of a flat universe or else the existence of spatial curvature.

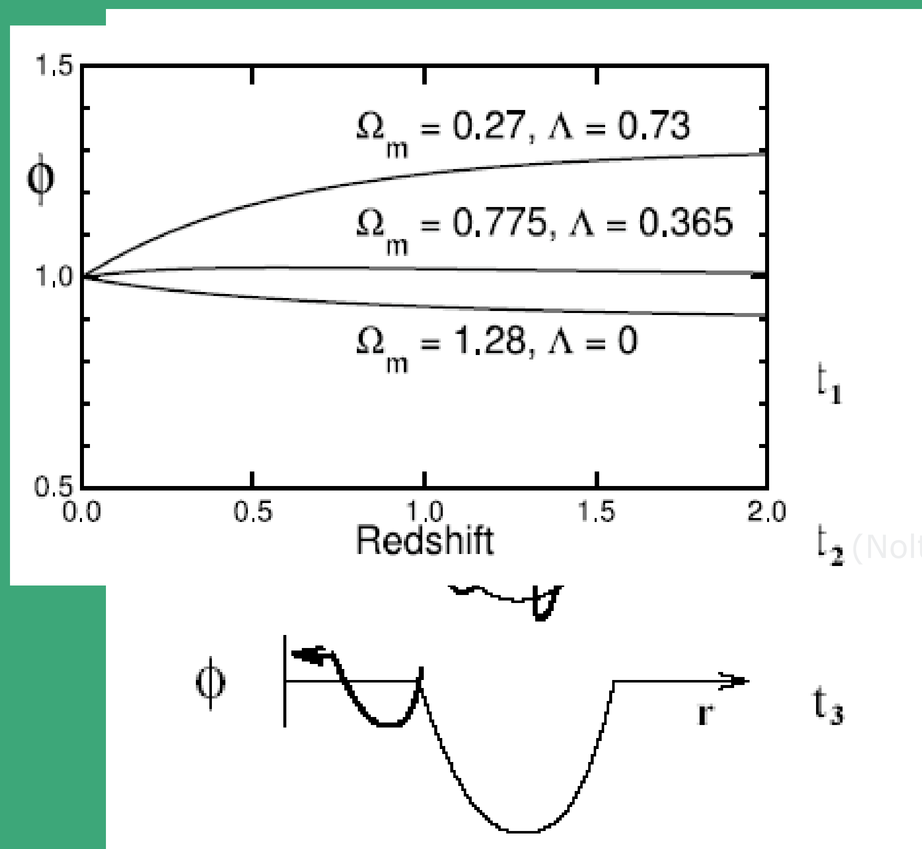

(Nolta et al. 2004)

RECENT DETECTIONS OF THE ISW EFFECT

• The time-varying potential influences both the CMB anisotropies (ISW effect) and the LSS distribution, which implies a non-null cross-correlation between the CMB and LSS maps.

• Several groups have reported ISW detection at different significant levels by cross-correlating WMAP with different LSS catalogues:

- Boughn & Crittenden (2004): HEAO-1, NVSS (2-2.5σ detection)
- Nolta et al. (2004): NVSS, 2.2σ detection, $\Omega_\Lambda > 0$ (95%)
- Fosalba and Gaztañaga (2004): APM, detection at 98.8%
- Fosalba, Gaztañaga & Castander (2004): SDSS, 3σ detection, $0.69 < \Omega_\Lambda < 0.86$ (2σ)
- Scranton et al. 2003 (astro-ph): SDSS-RLG, 2σ detection
- Afshordi et al. (2004): 2MASS, detection at 2.5σ
- Vielva, M-G, Tucci (2004): NVSS using spherical wavelets, >5σ detection

$$Cov^{theo}{}_{W-N}(R) = \sum_\ell \frac{2\ell+1}{4\pi} C_{\ell_M}(R)$$

$$C_{\ell_M}(R) = (p_\ell)^2 \, (s_\ell(R))^2 \, b_{W\,\ell} \, b_{N\,\ell} \, C_{\ell_{W-N}}$$

$$C_{\ell_{W-N}} = 12\pi\Omega_m H_o{}^2 \int \frac{dk}{k^3} \Delta_\delta{}^2(k) F_\ell{}^W(k) F_\ell{}^N(k),$$

$$\begin{aligned} F_\ell{}^W(k) &= \int dz \frac{dg}{dz} j_\ell(k\eta(z)) \\ F_\ell{}^N(k) &= b \int dz \frac{dN}{dz} D(z) j_\ell(k\eta(z)) \end{aligned}$$

NRAO VLA Sky Survey (NVSS)

- A survey of almost 2 million radio sources with a minimum flux of 2.5 mJy at 1.4 GHz covering about 80% of the sky (δ>-38°).
- We have represented the point sources in the HEALPix scheme at N_{side}=64 resolution (about 40 counts per pixel in average).
- The peak of the redshift distribution is expected to be at z~1 where the ISW effect is maximum.

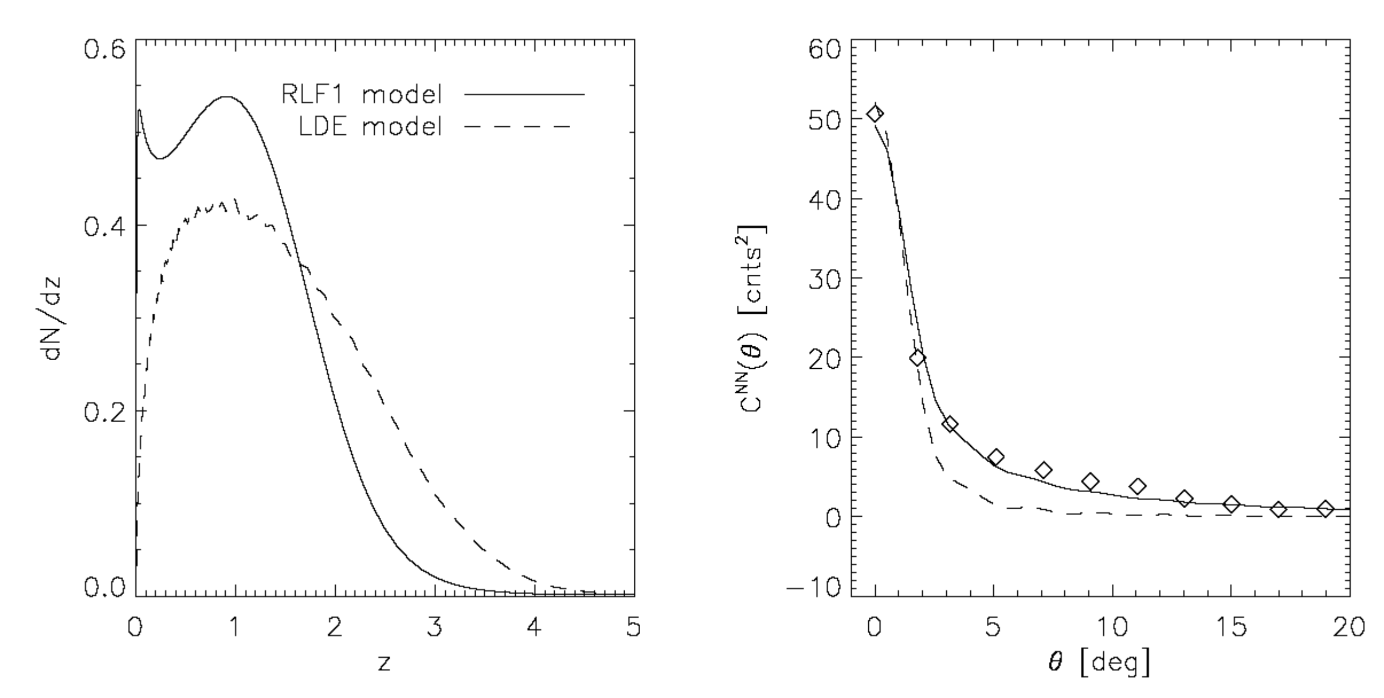

Vielva, M-G & Tucci 2004

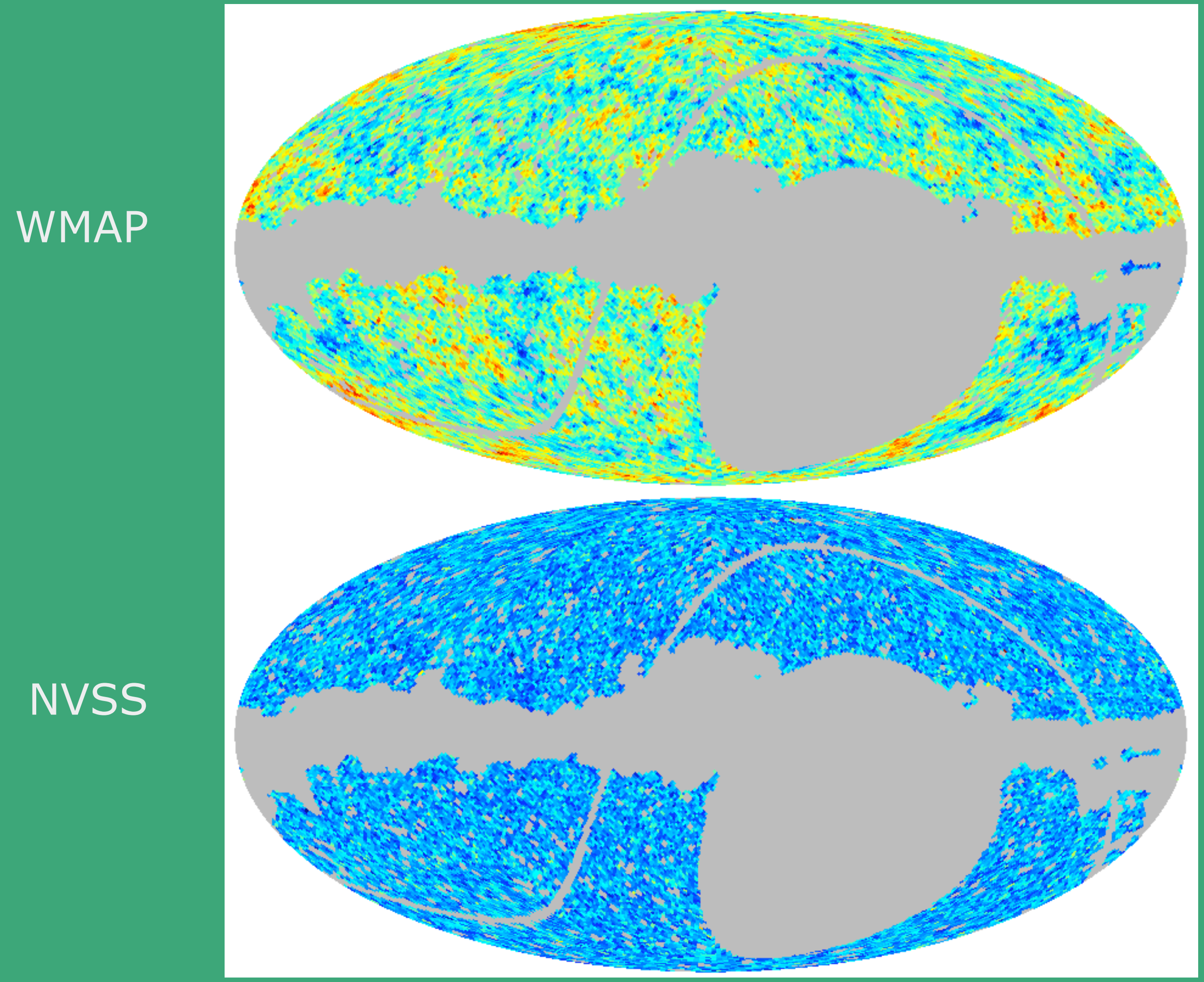

Vielva, M-G & Tucci 2004

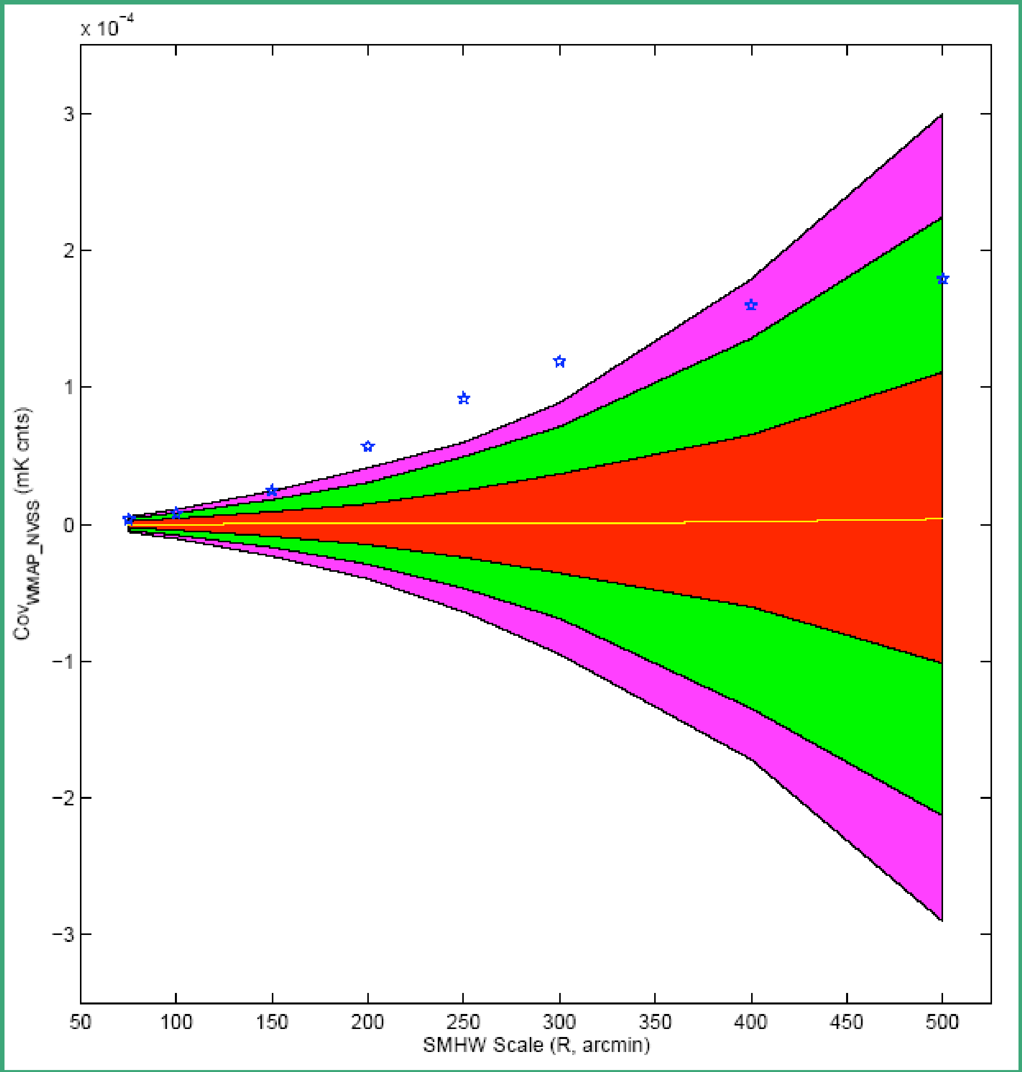

N-T Cross-Correlation

$$C^{NT}(\theta) < 2\sigma!!$$

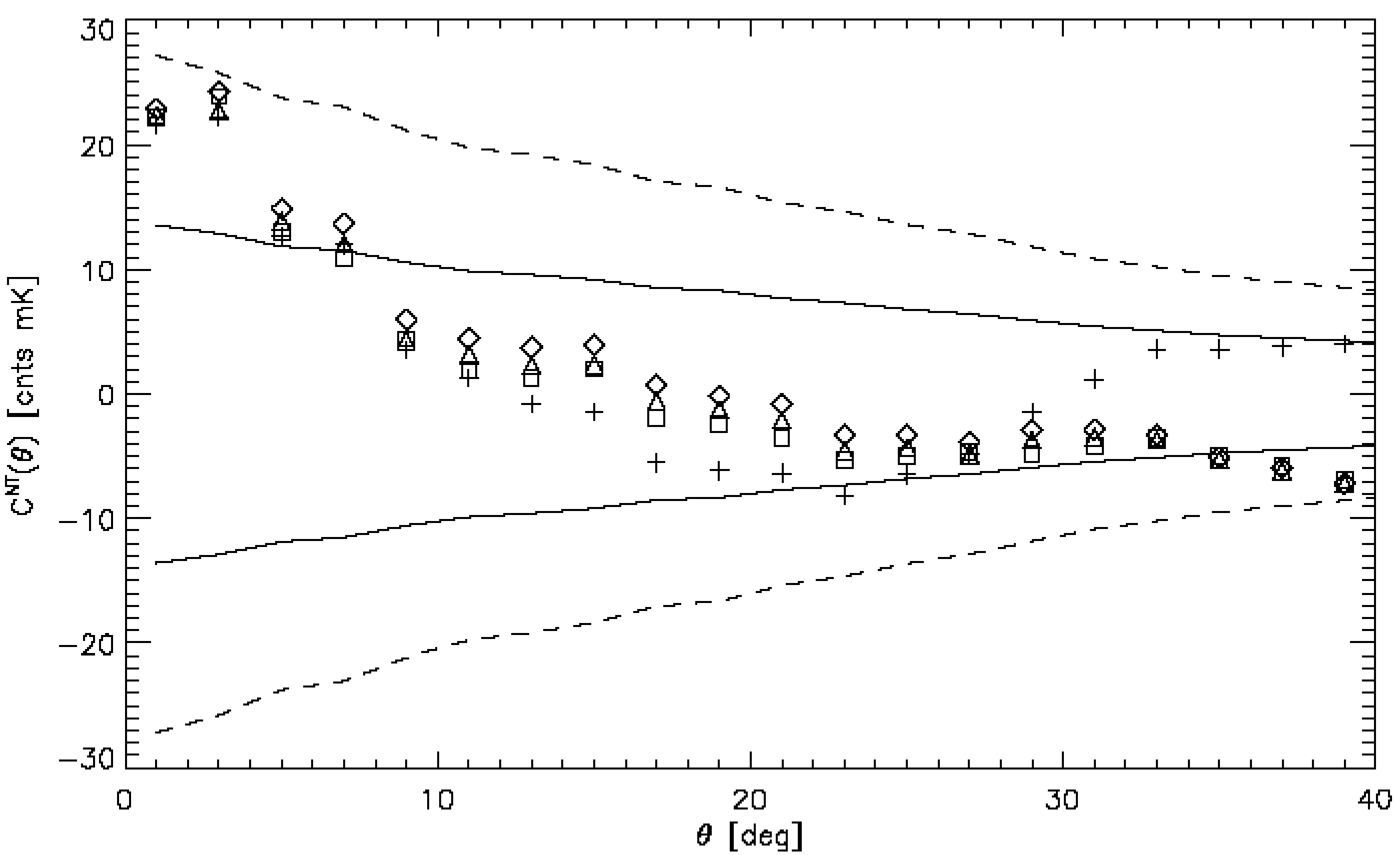

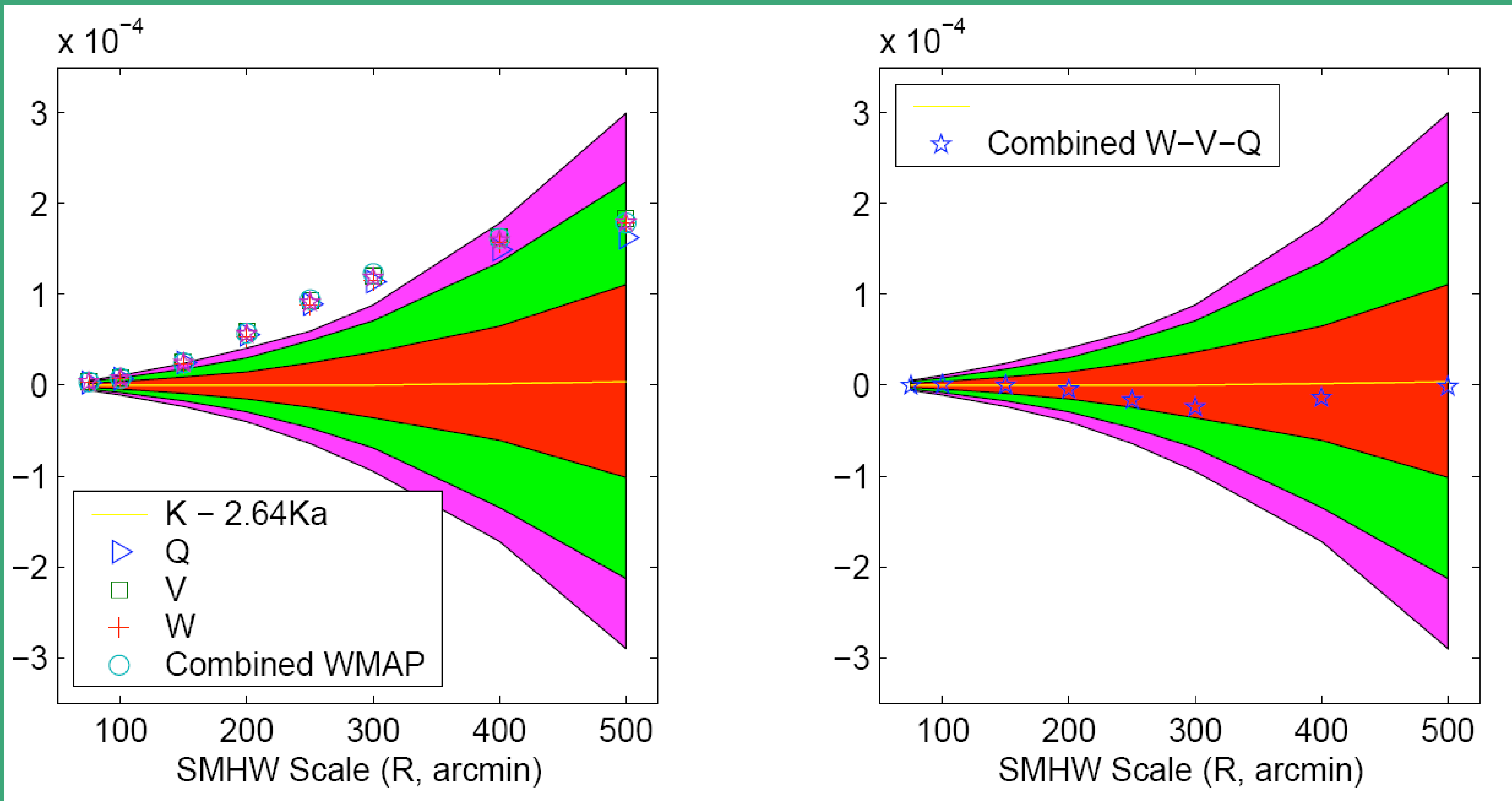

x 10^-4
3
2
1
0
−1
−2
−3
K − 2.64Ka
Q
V
W
Combined WMAP
100
200
300
400
500
SMHW Scale (R, arcmin)
x 10^-4
Combined W−V−Q
SMHW Scale (R, arcmin)

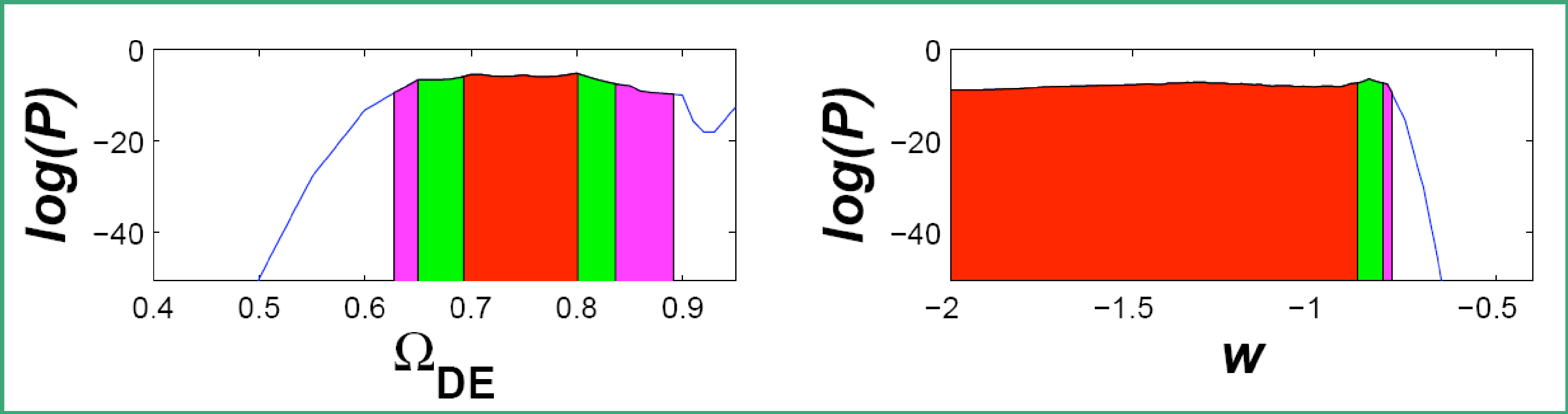

$0.69 < \Omega_\Lambda < 0.86$, $w < -0.81$ (2σ)